DNA Electronics, M. Di Ventra and M. Zwolak, in *Encyclopedia of Nanoscience and Nanotechnology*, H. Singh-Nalwa, Ed. (American Scientific Publishers, Stevenson Ranch, CA, 2004, Vol. 2, pp. 475–493)

ENN Encyclopedia of Nanoscience and Nanotechnology
www.aspbs.com/enn

DNA Electronics

Massimiliano Di Ventra, Michael Zwolak

Department of Physics, Virginia Polytechnic Institute and State University, Blacksburg, Virginia, USA

CONTENTS

1. INTRODUCTION

DNA, or deoxyribonucleic acid, encodes the architecture and function of cells in all living organisms. DNA, shown in Figure 1, is made of a sequence of four bases: thymine (T), cytosine (C), adenine (A), and guanine (G) (see Fig. 2 for a schematic of each base), attached to a phosphate-sugar backbone. Any particular sequence forms a single strand of DNA. Two strands may come together through hydrogen bonding of the bases A with T (AT) and G with C (GC). This forms the double helix structure discovered by Watson and Crick [1].

Apart from its fundamental role in defining the genetic code of living organisms, DNA's electronic and self-assembly properties have been the subject of much investigation over the past decade. Both properties bear enormous importance in understanding the functionalities of DNA in living cells and indicate that DNA could be of use in nanoscience. On the one hand, the transport properties of DNA are of interest in several disciplines because of their relevance to damage and mutation in DNA [2–13]. On the other hand, the use of molecules and nanomaterials to develop new ways of detecting, manipulating, and sequencing DNA is being pursued [14–25]. The charge transport properties of DNA are central to such developments. For instance, electrochemical detection of structural changes, due to protein binding or base mismatches, is currently being examined [26–34]. It has also been suggested that new read-out schemes on DNA chips [35], which can detect for the presence of different DNA sequences, might exploit the electronic properties of DNA [36]. Finally, understanding charge transport in DNA can shed new light on the transport properties of other systems with π–π interactions, that is, molecular crystals and discotic materials [37–39].

It was suggested early on that DNA could be a conductor because of the formation of a π-band across the different bases. Many researchers subsequently looked into this possibility [40–59]. π-stacking is important in the conducting properties of several other organic molecules [60–65]. In the early 1990s, the idea that DNA might conduct started to be pursued with more vigor. When Murphy et al. [66] suggested that electron transfer through DNA was responsible for fluorescence quenching of an excited molecule, intense debate was started over the charge transport properties of DNA [36, 67–100].

Since these early investigations, many researchers have looked at the transport properties of DNA and have found that it behaves as a conductor, semiconductor, or insulator, in what seems to be contradictory conclusions. The apparent contradictions have been attributed to the large phase space in which DNA can be prepared and probed (see, e.g., [36]). Many experimental conditions and attributes of the specific DNA used, including base sequence, length, orientation, counterions, temperature, electrode contact, adsorption surface, fluctuations, and so on, could affect its conducting properties. As a consequence, although much progress has been made, DNA's transport properties are still in question.

Despite the debate on whether DNA conducts or not, its self-assembly properties are being used to create novel nanoscale structures. For instance, silver wires and palladium wires were made using a DNA template [101, 102]. Devices that exploit DNA's complex properties are currently envisioned as transistors, biosensors, molecular memories, and complex circuits [103–114].

In this chapter, we will discuss the research done in understanding charge transport in DNA, and the novel electronic structures and devices that have been made using this important biological molecule. This chapter is organized as follows: in Section 2, we discuss the complex structure of DNA and the different DNA structures used in charge transport experiments. In Section 3, we review the experiments that try to identify the transport mechanism in DNA, both directly and indirectly, and the different theoretical interpretations

ISBN: 1-58883-001-2/$35.00

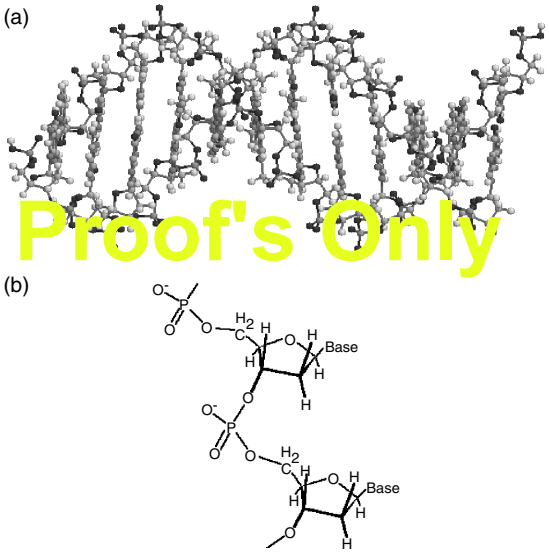

Figure 1. (a) DNA double helix. The DNA double helix is made of two strands, which are each a sequence of four bases attached to a phosphate-sugar backbone. The bases opposite each other on the two strands are bonded by hydrogen bonds. (b) Schematic of the chemical structure of the phosphate-sugar backbone of a single strand of DNA.

of charge transport that have been suggested over the years. Finally, in Section 4, we outline the possible applications of DNA in nanoscale electronics.

2. DNA STRUCTURE

DNA is a macromolecule made of four different monomers. Each monomer unit, called a nucleotide, consists of a phosphate group, a 2′-deoxyribose (a 5-carbon sugar), and one of four bases shown in Figure 2. The monomers are attached through a phosphodiester link. The pK_a of the phosphate group is near one, making it a strong acid. At physiological pH, it will therefore be negatively charged in solution. This charge is partially neutralized by counterions, such as sodium (Na^+), potassium (K^+), and magnesium (Mg^{2+}). Within the monomer, the 5′ and 3′ carbons are the carbons attached to the phosphate group on either side.

Polynucleotides (i.e., any sequence of single nucleotides) are actually thermodynamically unstable *in vivo* (in living organisms), that is, in an aqueous environment. The hydrolyzation of the linking oxygen, that is,

$$-O- + H_2O \longrightarrow -OH + HO-$$

in the phosphodiester group forms the individual monomer units, which are more stable. This process, however, is extremely slow without the presence of a catalyst. Nucleases are enzymes in living organisms which act as catalysts in this reaction to break down polynucleotides in food. It is common when directly measuring current–voltage (*I–V*) characteristics of DNA to use these enzymes to break DNA.

Double-stranded DNA is due to hydrogen bonding between bases on two single strands. In this case, the bases come together in what is called Watson–Crick base pairing. The A base only pairs with T, and the G base only pairs with C. These pairs allow for the formation of the double helix, a secondary structure of DNA (see Fig. 1). The carbons which bond to the phosphate-sugar backbone on each side of either base pair are the same distance apart, which allows for the regular structure of the helix.

In B-DNA, the common type of DNA found in cells of living organisms, the center of the base pairs lies along the helix axis. The helix is right handed. The base pairs are slightly tilted with respect to this axis and are separated by a distance of about 3.4 Å. This is close to the 3.3 Å in stacked phthalocyanines in which charge transport is perpendicular to the plane of the molecule [60]. There are, on average, 10 base pairs with each turn of the helix, which gives an average 36-degree angle between successive base pairs. However, the base-pair sequence and interaction with other molecules (e.g., counterions, proteins) can cause deviation from these average values.

Another form of DNA, A-DNA, is quite different from B-DNA; see Figure 3. In this structure, the base pairs are more tilted with respect to the helix axis. This should

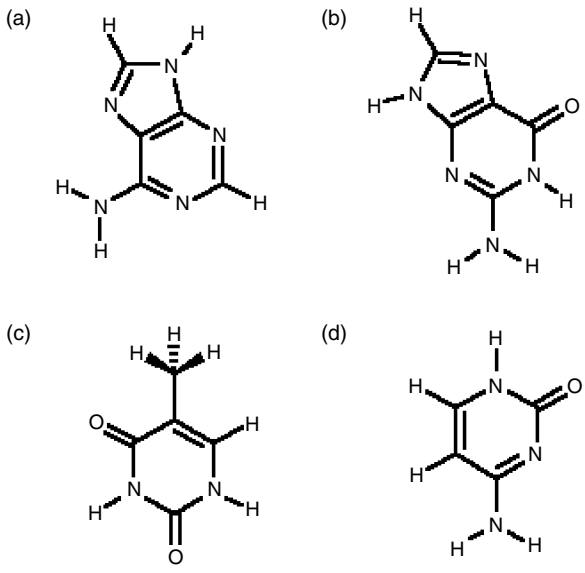

Figure 2. The four bases that compose DNA: (a) adenine, (b) guanine, (c) thymine, and (d) cytosine.

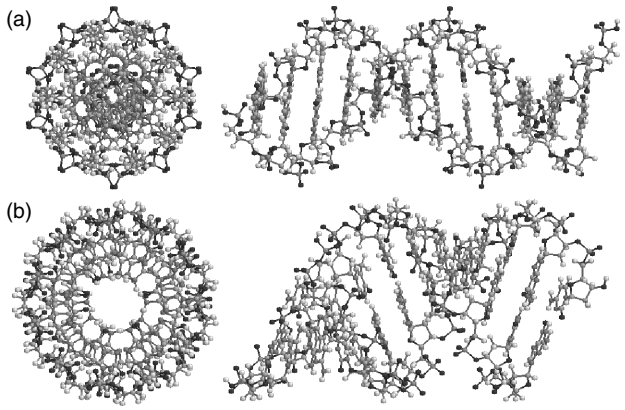

Figure 3. Top and side views of (a) B-DNA and (b) A-DNA.

significantly alter the electronic properties of DNA, especially if charge transport is through a π-channel [89]. The B-DNA is more stable than A-DNA in aqueous environments, due to water molecules that bind along the length of the chain. There are many other forms of DNA, including H-DNA, a triple helix whose formation is favored when there is a single strand of all purine bases (A and G) and a strand of all pyrimidine bases (C and T).

Single-stranded DNA has a mostly random structure. However, in some parts of the single strand there can be a secondary structure if self-complementary regions are present. In these regions, the DNA can pair up with itself and form a double helix.

A typical sequence of DNA used in charge transfer experiments is λ-DNA, which comes from a virus called Phage Lambda. The sequence consists of about 50,000 base pairs, which gives a length of about 16 μm. This is a complex sequence of DNA. Another natural sequence of DNA used in such experiments is calf-thymus DNA. Other common synthetic sequences of DNA are the homogeneous sequences, in which one strand is made of just one nucleotide and the other of its complement. These can either be poly(dG)–poly(dC) or poly(dA)–poly(dT). The DNA sequence can be cut to the length required in the experiment.

Finally, some experimental groups have used synthetic DNA hairpins to perform fluorescence and charge transfer measurements. Natural DNA hairpins are single strands of DNA which fold back onto themselves due to a self-complementary region. The synthetic DNA hairpins used are two short complementary polynucleotides linked with a fluorescent organic molecule, which stabilizes the structure.

3. CHARGE TRANSPORT IN DNA

3.1. Indirect Measurements of Charge Transport in DNA

In the early 1990s, Murphy et al. suggested that charge is transferred through DNA from an excited donor to an electron acceptor [66]. The donor and acceptor used in the experiment were metal complexes intercalated in a 15-base pair double-strand DNA. The intercalated donor complex was photoexcited in solution; in the absence of the acceptor, it would emit light. However, in the presence of the acceptor, the luminescence was found to be quenched at a high rate, suggesting that DNA carries charge from the donor to the acceptor. This was extraordinary since the estimated distance that charge was supposed to travel was about 4 nm.

In similar experiments, Brun and Harriman et al. used organic donors and acceptors [59, 115, 116]. They found that charge-transfer rates drop off fast as the length of the DNA increases; this is opposed to the findings of Murphy et al. [66]. Later on, Lincoln et al. conducted experiments with the metal complexes used by Murphy et al. [117] and modeled the data. The results suggested that the metal complexes must cooperatively bind onto the DNA, which explains the fast rate of charge transfer and its small "distance dependence" [117, 118]. After these reports, more experimental and theoretical research was done, adding to the seemingly contradictory results [96–100].

The contradictory results were attributed to various factors, including base sequence and how the charge was injected in the system (i.e., using intercalated metal complexes rather than intercalated organic molecules, etc.). More recent measurements [119, 120] were performed under more controlled conditions, and the sequence dependence of charge transfer has been systematically investigated. In many of these experiments, holes were injected into a GC pair; three GC pairs, with the G's on one strand (GGG), were the acceptors. The main findings are that DNA transfers charge over long distances of up to hundreds of angstroms [120]. However, the rate of transfer strongly depends on the base sequence. The rate of charge transfer between a hole injector (e.g., organic chromophore) and a GC pair, separated by a small number of AT pairs, drops off exponentially with the number of AT pairs. However, the rate stays relatively constant with increasing number of AT pairs when there are more than four AT pairs. This has been attributed to a change of transfer mechanism from coherent tunneling to hopping, which will be discussed in Section 3.3.

Henderson et al. covalently attached an anthraquinone derivative to a 60-base pair DNA oligomer [121]. The anthraquinone derivative was irradiated with ultraviolet light, which produces a radical cation on the GC pair attached to the quinone. The cation can then migrate down the length of DNA, where there are GG sequences in several places. The location of the charge can be detected as strand scission at these places with treatment of piperidine. This yields an exponential dependence of the charge transfer up to about 18 nm of DNA length, with a very large decay length.

Using stilbenedicarboxamide (SA) linked to a DNA hairpin, Lewis et al. examined the distance dependence of charge transfer [73]. The experiment consisted of attaching SA to the end of one sequence of T's and one sequence of A's. A GC pair was substituted for one of the AT pairs. This GC pair behaved as an acceptor. It was found that, if the GC pair was directly attached to the SA, the fluorescence of the photoexcited SA was quenched. If the GC pair moved away from the SA, the quenching rate decreased. When the GC pair had four AT pairs separating it from the SA, there would be very little quenching. This suggests a strong distance dependence of the quenching rate when there are a few AT pairs separating the donor and acceptor. However, it was found that if there are long sequences of DNA with only AT pairs, there would be thermal hopping through the AT bridge. The A base would carry the holes since it has the second smallest ionization potential [122]. Giese et al. observed that the amount of charge on a GGG triplet transferred across a bridge of n AT pairs decreases rapidly as the number of AT pairs increases from one to three [123]. However, a further increase in the number of AT pairs would only slightly reduce the amount of charge transferred [123–125]. This can be explained by the formation of the highest occupied molecular orbital band across the AT pairs, which lowers the energy barrier for hole transfer. We will discuss this mechanism in more detail in Section 3.3.

More recently, contactless measurements of the conducting properties of DNA have indicated that this molecule is not a conductor [126–130]. These experiments have been designed to minimize contact effects. The contacts could

be the source of high resistance observed in direct measurements [128]. These experiments were done by adsorbing both DNA and single-walled nanotubes on different insulating substrates. A gold electrode was then evaporated on part of the substrate. Using a scanning force microscope (SFM) tip, the DNA molecules were imaged near the electrode. The same area was reimaged with a voltage of 1.6 V applied to the tip. The nanotubes contrasted more intensely to the substrate due to electrostatic interaction. However, no additional contrast was seen in the case of λ-DNA or poly(dG)–poly(dC). DNA molecules that were not partly covered by the gold electrode, but were in contact with a nanotube, were also imaged. No additional contrast was seen in this case either. Using an oscillating SFM tip, the single-walled nanotubes and the DNA with no electrode were also scanned [128]. In this process, the frequency of the SFM tip oscillations should decrease if the specimen is conducting, due to the polarization of the sample. The decrease in frequency was actually observed for the nanotubes, but not for DNA, suggesting that the molecule behaves as an insulator [128]. However, in this case, the insulating character of DNA could be due to distortions caused by the substrate.

In another indirect measurement, Tran et al. measured the resistance of λ-DNA via the change in the quality factor of a resonant cavity when the DNA is placed in it [130]. The λ-DNA has been found to have a conductivity on the order of 1 $(\Omega\ \mathrm{cm})^{-1}$ or, assuming a DNA diameter of 2 nm, a resistance of about $10^{10}\ \Omega$ for the full length λ-DNA (∼16 μm).

3.2. Direct Measurements of Current–Voltage Characteristics

Fink and Schonenberger performed the first direct measurement of the conducting properties of DNA [131, 132]. The resulting *I–V* characteristics are shown in Figure 4. It was found that λ-DNA is a good conductor, with a resistance comparable to that of conducting polymers. The experiment was done in vacuum, where a drop of solution containing DNA was placed onto a gold-covered carbon foil with 2 μm holes. Excess solution was removed with blotting paper. The holes were imaged with a low-energy electron point source (LEEPS) microscope, which is claimed to not radiatively damage DNA [131, 133]. Upon scanning, holes were occasionally found with only one DNA rope (e.g., several DNA molecules twisted together) spanning across it. The DNA ropes were then broken by using a tungsten tip. The tip was also used to apply a bias across the DNA. A 600 nm portion of a DNA rope produced a resistance of 2.5 MΩ. This provides an upper value for the resistance of DNA, since some finite contact resistance is expected to contribute. Since the experiment was done in vacuum, ionic conduction could not account for the transfer mechanism. However, this experiment does not rule out that ions trapped by the DNA might have changed its electronic structure, allowing for higher conductivity. There has also been some evidence that LEEPS imaging contaminates the DNA and can account for the conducting behavior observed in this experiment [134].

In other direct measurements, researchers have found that DNA acts as a large bandgap semiconductor. For

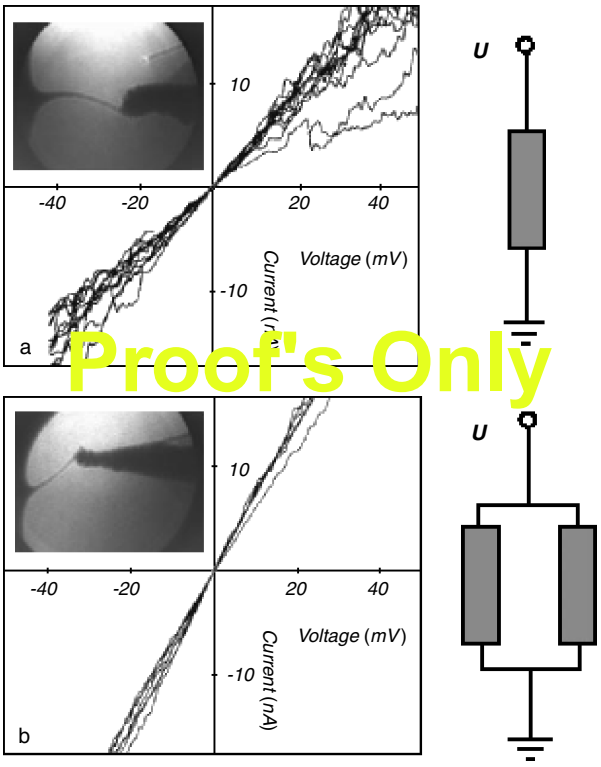

Figure 4. *I–V* characteristics of DNA ropes. (a) *I–V* curve for a single rope 600 nm long. The inset shows the LEEPS image of DNA rope attached to a tungsten tip. (b) *I–V* curve for two ropes in parallel. The inset shows the LEEPS image of the DNA ropes attached to the tungsten tip. Reprinted with permission from [131], H.-W. Fink and C. Schonenberger, *Nature* (*London*) 398, 407 (1999). © 1999, Nature Publishing Group.

instance, Porath et al. measured the conductivity in poly(dG)–poly(dC) DNA [135]. The homogeneous sequence is ideal for overlap of π-orbitals in adjacent base pairs. These experiments were done using a DNA oligomer 30 base pairs long or, equivalently, 10.4 nm long. An electrostatically trapping technique [136, 137] was used to position single DNA molecules between two electrodes 8 nm apart (see Fig. 5). The sample was then dried with a flow of nitrogen. The *I–V* characteristics of this experiment are shown in Figure 5. As is clear from Figure 5, the DNA oligomer does not conduct charge for biases below about 1 V at room temperature, which shows that poly(dG)–poly(dC) DNA behaves like a semiconductor with a large bandgap. As in previous measurements, these results do not rule out the possibility that ions could be attached to the DNA, thus modifying its electronic structure. In Section 3.3, we discuss the possibility that the DNA backbone could induce the semiconducting behavior.

Watanabe et al. measured charge transfer in a single DNA molecule from a biological source using an atomic force microscope (AFM) with a carbon nanotube tip and a two-probe "nanotweezer" made with two multiwalled carbon nanotubes, shown in Figure 6a [138]. Vibrating the two probes of the nanotweezer ensured that the probes did not adhere to each other or the sample. Watanabe et al. reported that the probes could be positioned with roughly 2 nm accuracy. The DNA was deposited on a

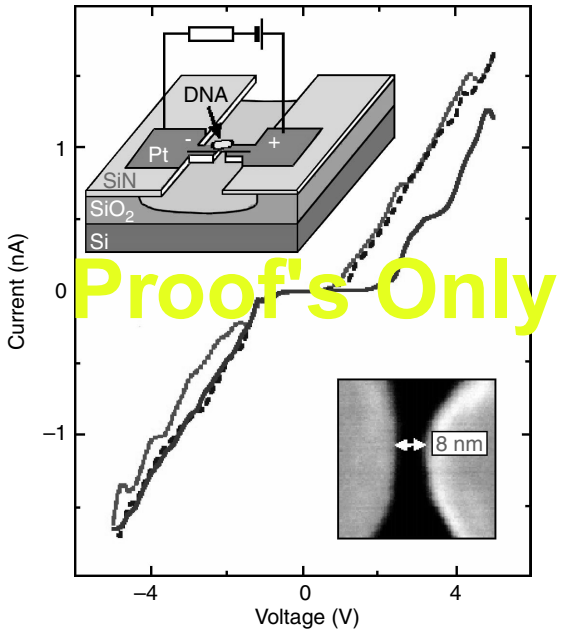

Figure 5. *I–V* characteristics for single poly(dG)–poly(dC) DNA molecules. The different curves show repeated measurements. The upper inset shows the experimental setup. The lower inset shows the electrodes separated by a 8 nm gap. Reprinted with permission from [135], D. Porath et al., *Nature* (*London*) 403, 635 (2000). © 2000, Nature Publishing Group.

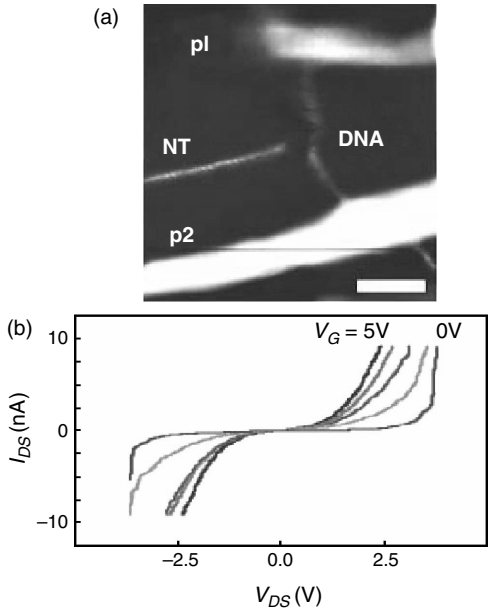

Figure 6. (a) AFM image (scale bar, 10 nm) of the experimental setup. p1 is the source and p2 the drain of the two-probe nanotweezer. NT is the carbon nanotube used to apply the gate voltage. (b) *I–V* characteristics of biological DNA at different gate voltages, V_G. Reprinted with permission from [138], H. Watanabe et al., *Appl. Phys. Lett.* 79, 2462 (2001). © 2001, American Institute of Physics.

SiO_2/Si(100) surface and dried under a flow of nitrogen gas. Afterwards, the sample was kept in a nitrogen atmosphere. Figure 6b shows the *I–V* characteristics at room temperature for a 25 nm separation of the source and drain. The measurements in Figure 6b indicate that double-strand DNA is semiconducting with a voltage gap of about 2 V. Applying a gate voltage with the carbon nanotube tip reduces this gap significantly. Figure 7 shows the *I–V* characteristics at room temperature if the carbon nanotube tip is placed across the DNA molecule. The tip is held at 2 V. A Coulomb blockade-like staircase is observed whose origin is still unclear.

Hwang et al. made direct measurements using gold electrodes on a SiO_2 substrate [139, 140]. A drop of a solution of 60 base pair poly(dG)–poly(dC) DNA was deposited between the electrodes and then dried with nitrogen gas. Almost linear *I–V* characteristics were found with electrodes separated by a 30 μm gap. However, when the electrode gap was reduced to 20 nm, highly nonlinear *I–V* characteristics and a large voltage gap were found.

De Pablo et al. recently performed measurements on the resistance of λ-DNA by depositing DNA on a mica surface next to a gold electrode. A gold-covered SFM tip was positioned close to one of the DNA chains to function as a second contact. Using the SFM tip at different distances from the electrode, a lower resistivity limit of 10^4 Ω cm was found for a DNA molecule. The same authors reported a lower resistivity limit of 10^6 Ω cm for a DNA molecule using a different method. These results suggest that λ-DNA is an insulator. This is in clear contradiction with previous results obtained by Fink and Schonenberger [131]. De Pablo et al. [134] suggest that the disagreement could be due to the effect of the low-energy electron beam Fink and Schonenberger use to image the DNA ropes [131]. In order to prove this, de Pablo et al. irradiated their samples in a vacuum with a low-energy electron beam and found that the DNA resistivity is greatly reduced after irradiation [134]. SFM images show that the sample had indeed been contaminated by the electron beam.

Kasumov and Klinov [141] offered another possible explanation for the discrepancy. These authors suggest that the compression induced by depositing DNA on surfaces changes its electronic structure. By depositing λ-DNA on a mica substrate partially covered with platinum, Kasumov and Klinov found, by simultaneously measuring the DNA height and conductivity using an AFM, that DNA did not conduct and its height was 1 nm. However, if pentylamine vapor was diffused on the Pt/mica surface before depositing the DNA, its height was found to be about 2 nm. At the same time, the DNA was found to conduct. The authors explained this observation by the reduction of the interaction of the mica substrate with the DNA after vapor discharge. Other studies seem to support the finding that the DNA height changes on different substrates [142].

The change in conductivity due to the different compressions can be explained as follows: If the charge transport relies on a very organized DNA chain (i.e., if the transport is through the π-channel), then compression will disrupt the π-channel greatly. The compression could be of such a magnitude that the single strands in the DNA duplex are essentially independent, a case which is believed to lead to small conductivity [92].

Storm et al. measured the conductivity of single DNA molecules and bundles of DNA molecules, finding for mixed-sequence, 1.5 μm long, DNA molecules on a SiO_2 surface between two gold electrodes about 300 nm apart a

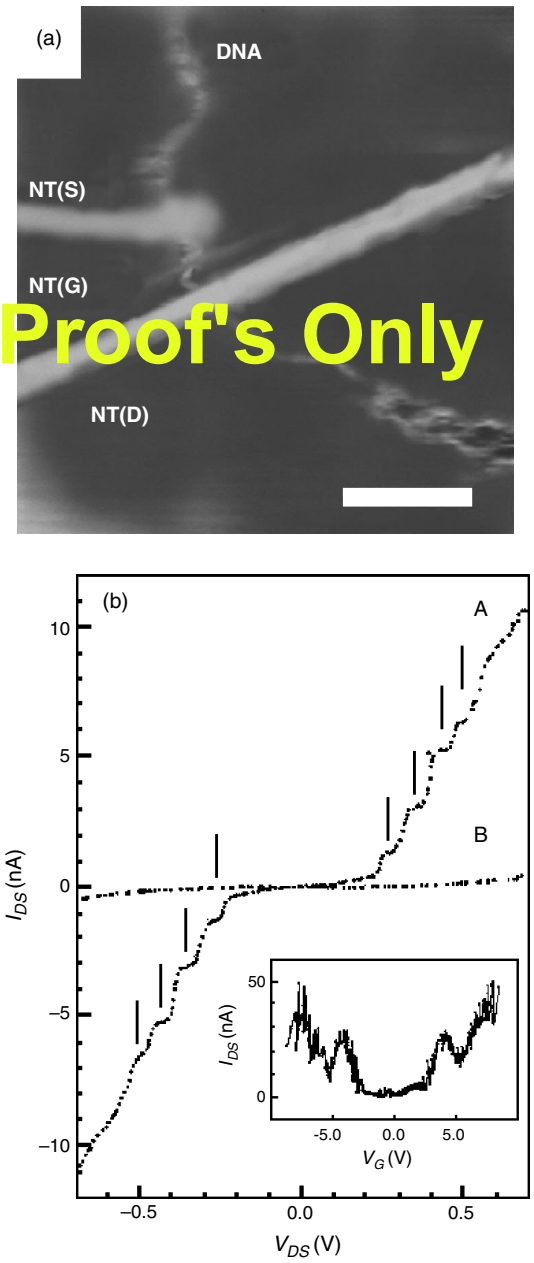

Figure 7. (a) AFM image (scale bar, 10 nm) of the experimental setup. The nanotube gate, NT(G), is placed across the DNA molecule. The source, NT(S), and drain, NT(D), are separated by 5 nm. (b) *I–V* characteristics when the carbon nanotube tip is placed across the DNA molecule. The inset shows the current versus the gate voltage at a source-drain voltage of 0.5 V. Reprinted with permission from [138], H. Watanabe et al., *Appl. Phys. Lett.* 79, 2462 (2001). © 2001, American Institute of Physics.

lower resistance limit of 10 TΩ for about 10 molecules in parallel [143]. These measurements were done at ambient conditions. The DNA was bonded to the electrodes through a thiol group. Other samples with different electrode spacing also showed large resistance. However, the DNA height was measured to be 0.5 nm, suggesting that the compression induced by the surface may play a prominent role in decreasing the conductivity in this case. A similar device made of a mixed-sequence, 300 nm long DNA, and platinum electrodes at a distance of 40 nm on a SiO_2 substrate, also showed a resistance of 10 TΩ. Finally, poly(dG)–poly(dC) DNA with no thiol groups showed resistances greater than 1 TΩ on both SiO_2 and mica substrates.

Yoo et al. measured the conductance in poly(dG)–poly(dC) and poly(dA)–poly(dT) DNA [144]. Poly(dG)–poly(dC) DNA 1.7–2.9 μm long and poly(dA)–poly(dT) DNA 0.5–1.5 μm long were used in the experiments. DNA was electrostatically trapped [137] between electrodes 20 nm apart and dried with nitrogen. Measurements at both ambient conditions and in a vacuum were performed, with no substantial change in the results. The *I–V* characteristics for poly(dA)–poly(dT) DNA showed a large bandgap at temperatures lower than 161 K. A strong temperature dependence of the current was also observed [144]. This can be accounted for by a small polaron hopping model [145], where the current is given by

$$I \propto \sinh bV \exp(-E_a/k_B T) \tag{1}$$

where E_a is the activation energy, T is the background temperature, $b = ea/2k_B Td$, e is the electron charge, a is the hopping distance, and d is the distance between the electrodes. Equation (1) describes the *I–V* characteristics of poly(dA)–poly(dT) DNA very well if b is taken to be independent of temperature. Poly(dG)–poly(dC) DNA displays similar temperature behavior to that of poly(dA)–poly(dT) DNA, but with a much lower resistance of 1.3 MΩ at room temperature compared to 100 MΩ for poly(dA)–poly(dT) DNA. Poly(dG)–poly(dC) DNA shows the correct temperature dependence of b. Furthermore, poly(dG)–poly(dC) DNA shows temperature dependence of the current down to 4.2 K and seems to have two molecular vibration frequencies which contribute to the polaron motion, whereas poly(dA)–poly(dT) DNA shows temperature dependence only down to 50 K and seems to support only one molecular vibration.

Yoo et al. also performed *I–V* measurements with a gate bias [144] and found that poly(dA)–poly(dT) DNA has larger conductance upon application of a positive gate voltage, while poly(dG)–poly(dC) DNA has enhanced conductance under negative gate voltage conditions. Thus, in these experiments, poly(dA)–poly(dT) DNA displays *n*-type conducting behavior, while poly(dG)–poly(dC) DNA displays *p*-type behavior.

In addition to semiconducting and insulating behavior, Kasumov et al. reported proximity-induced superconductivity (i.e., superconductivity induced by the nearby electrodes) in DNA [146]. Using sputtering techniques, Kasumov et al. deposited rhenium/carbon electrodes on a freshly cleaved mica surface [146]. The rhenium layer was 2 nm thick, and the carbon layer developed into clumps (see Fig. 8). A flow of 16 μm long λ-DNA solution parallel to the electrodes introduced about 100 to 200 DNA molecules bridging the gap between the electrodes.

The overall resistance of the structure decreased from 1 GΩ, with no DNA molecules deposited, to a few kΩ after deposition (or a few hundred ohms per DNA molecule). The structure showed no decrease in resistance when treated with the buffer solution without the DNA. Kasumov et al. used a low-powered focused laser beam to destroy

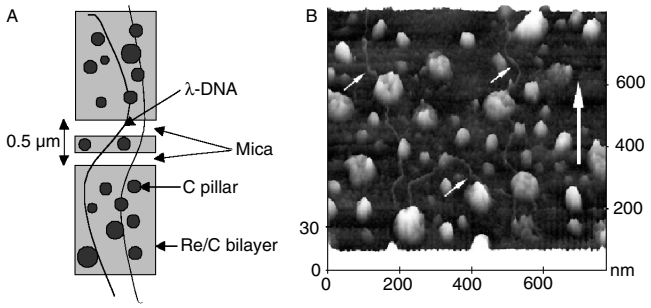

Figure 8. (a) A schematic of the rhenium/carbon electrodes. (b) AFM image of the Re/C film with deposited DNA molecules. The small arrows show the DNA molecules and the large arrow shows the direction of the solution flow. Reprinted with permission from [146], A. Yu. Kasumov et al., *Science* 291, 280 (2001). © 2001, The American Association for the Advancement of Science.

DNA molecules within the gap, except for in a narrow portion. In this way, three different samples were obtained with approximately 10 DNA chains (DNA1), 40 DNA chains (DNA2), and 2–3 DNA chains (DNA3), respectively. The resistance of all three samples increased as the temperature decreased. However, DNA1 and DNA2 decreased in resistance below the superconducting transition of the electrodes (see Fig. 9). The application of a magnetic field increased the resistance at temperatures close to the superconducting transition, which is the case for proximity-induced superconductivity [146]. The DNA3 sample showed an increased resistance even below the superconducting transition and a decreased resistance with increasing magnetic field, suggesting that this was not a case of proximity-induced superconductivity [146]. In order to prove that these unusual conducting properties are attributable to DNA bridging the electrodes, the samples were reheated to room temperature and treated with a flow of buffer solution for about 30 minutes. This did not result in a change of resistance. When DNase was added, however, the resistance increased back to that of the original electrode systems (without the DNA), showing that the transport was indeed taking place through the DNA molecule.

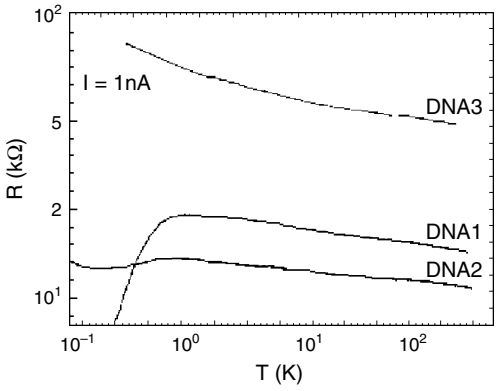

Figure 9. Resistance measurements as a function of temperature for λ-DNA between superconducting electrodes for the three samples discussed in the text. Reprinted with permission from [146], A. Yu. Kasumov et al., *Science* 291, 280 (2001). © 2001, The American Association for the Advancement of Science.

Although not conclusive, the results of Kasumov et al. show that proximity-induced superconductivity can be realized in DNA, and that thermal hopping is an unlikely mechanism of transport in λ-DNA, since the resistance does not increase strongly with decreasing temperature.

Other researchers have measured conductivity in DNA networks. Cai et al., for instance, investigated networks of poly(dG)–poly(dC) DNA and networks of poly(dA)–poly(dT) DNA self-assembled onto a mica surface (see Fig. 10) [147]. The samples were made of a drop of a DNA solution adsorbed onto a freshly cleaved mica surface and incubated for about one minute. The excess solution was then removed and dried with a flow of nitrogen gas. The sample was also kept under vacuum conditions for 5 to 12 hours, after which the electrical characteristics were measured. The poly(dG)–poly(dC) DNA networks show a "uniform reticulated structure" opposed to poly(dA)–poly(dT) DNA which forms a cross-linked network. Details of these structures can also be controlled [148–150]. A gold electrode was evaporated to form a contact to the DNA network, as shown in Figure 10c and d. Using a conducting probe AFM, Cai et al. measured the *I–V* characteristics of these networks. Without DNA, a noise of about 1 pA was measured. Placing the AFM tip 100 nm away from the gold electrodes (see Fig. 11a), the current in poly(dG)–poly(dC) DNA displayed ohmic behavior. Poly(dG)–poly(dC) DNA also exhibited *p*-type rectifying behavior (see Fig. 11d). Poly(dA)–poly(dT) DNA, on the other hand, displayed much higher resistances. However, in this case as well, ions from the buffer solution could have changed the electronic properties of the DNA.

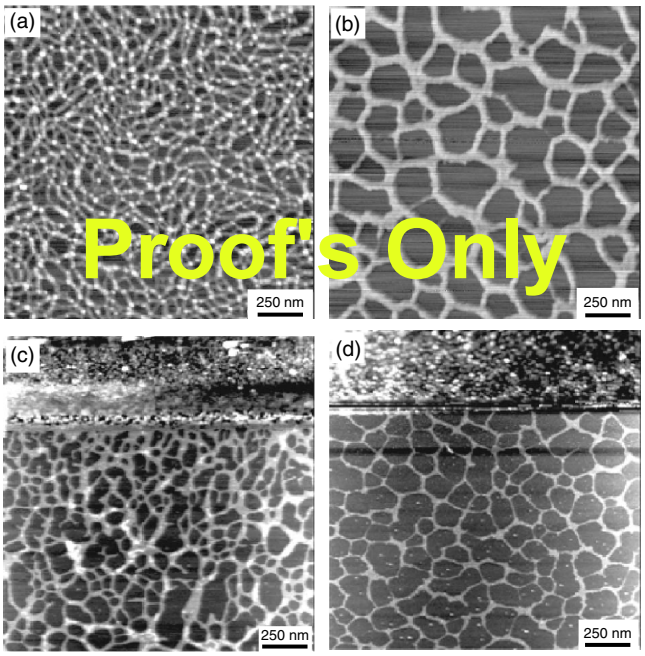

Figure 10. AFM images of self-assembled networks of (a) poly(dA)–poly(dT) DNA and (b) poly(dG)–poly(dC) DNA. (c) Poly(dA)–poly(dT) DNA with a gold electrode and (d) poly(dG)–poly(dC) DNA with a gold electrode. Reprinted with permission from [147], L. Cai et al., *Appl. Phys. Lett.* 77, 3105 (2000). © 2001, American Institute of Physics.

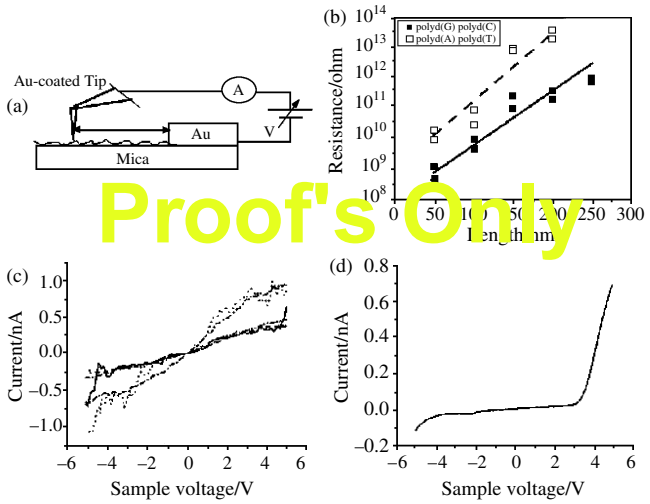

Figure 11. (a) Experimental setup. (b) Resistance versus length for poly(dG)–poly(dC) DNA and poly(dA)–poly(dT) DNA. (c) *I–V* characteristics for poly(dG)–poly(dC) DNA. (d) Rectifying curve for poly(dG)–poly(dC) DNA. Reprinted with permission from [147], L. Cai et al., *Appl. Phys. Lett.* 77, 3105 (2000). © 2001, American Institute of Physics.

Zhang et al. [151] recently focused on eliminating, or at least reducing, two experimental factors, contact resistance [152, 153] and ions from the solutions, which could have caused the large discrepancy between previous experimental results. Such direct measurements indicate that DNA is generally insulating. λ-DNA on a quartz substrate between 4 μm thick gold electrodes was used in these experiments. The DNA ends were modified to include a T base with a thiol group, so that the base could easily bind to the gold electrodes. The electrode distance was fixed at 4 or 8 μm. A solution of DNA molecules was applied to the electrodes and then diffused across the electrodes by a flow of solution. Mg^{2+} ions were introduced so that the DNA could stick to the quartz surface while it was rinsed with NH_4Ac to remove leftover salt from the buffer solution. The volatile NH_4Ac was then removed under vacuum. The corresponding *I–V* characteristics showed no conduction for an applied voltage of up to 20 V for λ-DNA between electrodes 4 μm apart. A lower resistivity limit of 10^6 Ω cm was found for biases up to 20 V.

These results suggest that the lower resistivities measured by other groups are due to ionic contamination from the buffer solution and/or from other sources. The influence of ions and humidity on both the structure and the electronic properties of DNA has also been intensively studied by other researchers [154, 155]. Lee et al. did experiments to examine the influence of both humidity and oxygen on the conductance properties of DNA [155]. Trapped oxygen has been found to dope poly(dG)–poly(dC) DNA with holes and increase its conductivity. In these experiments, 1.7–2.9 μm poly(dG)–poly(dC) DNA and 0.5–1.5 μm poly(dA)–poly(dC) DNA were placed between Au/Ti electrodes. The distance between the electrodes varied between 100 to 200 nm. A DNA solution was dropped between the electrodes and allowed to dry. *I–V* curves were measured under three conditions: in air with 35% humidity, in an oxygen–nitrogen (1:4 ratio) atmosphere with less than 0.1% humidity, and in a vacuum. For poly(dG)–poly(dC) DNA at 1 V, the resistance increased from about 0.8 to 7 to 100 GΩ, for the three different conditions, respectively. Finally, when poly(dG)–poly(dC) DNA was exposed to pure oxygen gas instead of air, the conductance increased by over 100 times. This shows that oxygen doping has a larger impact on the DNA resistance than water. In the case of poly(dA)–poly(dT) DNA, the conduction decreased when the sample was placed in a pure oxygen atmosphere. These results also support early findings that poly(dG)–poly(dC) DNA is a *p*-type conductor and poly(dA)–poly(dT) DNA is an *n*-type conductor [144, 147].

3.3. Charge Transport Mechanisms

The previous section reviewed the main experiments on the transport properties of DNA, showing that in several instances these experiments yielded contradictory results, even on supposedly similar system configurations. This section focuses on the interpretation of these experiments on the basis of physical models. Over the past several years, many transport mechanisms have been proposed to account for differing experimental results. This does not come as a surprise due to the wide range of conducting properties found for DNA. Specifically, three possible mechanisms for charge transport stand as the main physical processes: thermal hopping, sequential tunneling, and coherent tunneling (see Fig. 12). Polaron and soliton formation and transport have also been investigated and will be discussed at the end of this section.

In certain experiments, some of the three main mechanisms can be ruled out on the basis of the DNA configuration or experimental conditions. For instance, in the fluorescence experiments, charge could thermally hop from base to base (see Fig. 12A). However, the thermal energy required for this process is generally quite large; thus, this mechanism is unlikely in this case, as in many other cases. Charge can also sequentially tunnel from one site to the next (see Fig. 12B). After each tunneling process the coherence of the charge wavefunction is lost through dephasing processes, such as scattering with molecular vibrations. Neither of these mechanisms depends strongly on the DNA length. Finally, charge can tunnel through a whole length of DNA (see Fig. 12C). In this case, the charge wavefunction does not lose phase coherence, so the process is called coherent or unistep tunneling. This mechanism has a strong distance dependence. In the case of DNA, many researchers have

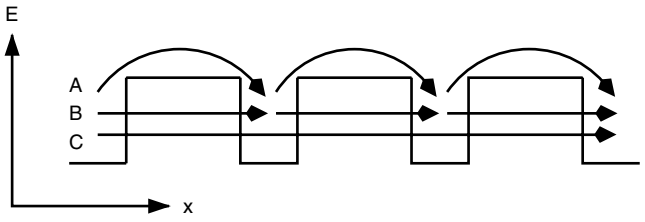

Figure 12. Schematic of three possible mechanisms for charge transfer in DNA, depicted as a series of energy barriers, (A) thermal hopping, (B) sequential tunneling, and (C) coherent or unistep tunneling. The vertical axis represents energy, *E*, and the horizontal axis represents the spatial position, *x*.

assumed that charge coherently tunnels through the whole length of DNA, with a rate of charge transfer R,

$$R \propto \exp(-\beta L) \tag{2}$$

where L is the length of the DNA and β is the tunneling decay length. A large value of β means that the rate of tunneling will decrease rapidly with increasing distance. However, earlier measurements yielded seemingly contradictory values for β [96–100].

Charge transport over large distances by a single tunneling step is unlikely. Theoretical studies have shown that the rate of coherent tunneling should drop off dramatically with distance [156]. Thus, many argue that sequential tunneling is the most likely mechanism for charge transport in DNA. Within this mechanism, holes have been studied as the likely charge carrier. The G base is the most favorable site for location of holes due to the order of the ionization potentials (G < A < C < T), which is independent of nearest neighbor bases [122, 157–169]. Many models have looked into the possibility of hole transport via G bases, along with other mechanisms of charge transport [170–194].

Berlin et al. did a quantitative analysis of sequential tunneling using kinetic rate equations [171, 172]. In this work, sequential tunneling between GC pairs through a bridge of AT pairs has been studied. A G^+ radical is considered as the charge donor and the base sequence GGG as the acceptor, in close connection with the experiments by Meggers et al. [75] and Giese et al. [195]. The base sequence GGG acts as an acceptor due to the lower ionization potential compared to a single G base. The ratios of reaction yields of water between the GGG site to the first G site, and also the GGG site with all the other G sites, were calculated. Tunneling rates from short DNA chains were taken from theory and experiment [75, 188, 195] and used to calculate the ratio of reaction yields for different base sequences. A fair amount of agreement with experiments has been obtained [75, 195]. Berlin et al. found that the rate for sequential tunneling drops exponentially with distance due to the reaction with water. The β parameter was found to be 0.1 $Å^{-1}$ for sequential tunneling, compared to a value of about 1 $Å^{-1}$ for coherent tunneling [156].

The physical meaning of the model is as follows. A hole is generated on some G base (part of a GC pair) to obtain a G^+ radical. The hole is then assumed to hop along the length of DNA to successive G bases, or, alternatively, the G^+ radical can undergo a reaction with water. If there are some sites with a sequence of many G bases (i.e., GG...G), then the hole is assumed to be transferred to the first G base to obtain (G^+G...G). This electronic configuration can relax to the lower energy state $(GG...G)^+$, trapping the hole. Alternatively, the hole can transfer to adjacent single G bases along the length of the DNA. If the time to relax from the configuration (G^+G...G) to the more stable $(GG...G)^+$ is small, the hole travels along the DNA until it reaches a GG...G site, where it is trapped. On the other hand, if the relaxation time is large, the hole will continue to travel along the DNA without being trapped. The first possibility seems to explain the experimental data of [75, 195].

Berlin et al. [174] also studied the competition between coherent and hopping transport using a one-dimensional tight-binding model. In this model, the DNA sequence was chosen to be of the form $(AT)_m$–GC–$(AT)_n$–GC–$(AT)_m$. The rate for tunneling was assumed to be

$$\nu_{\text{tun}} \exp(-\beta L) \tag{3}$$

where $L = (n + 1)a$ is the distance between the two GC pairs, n is the number of AT pairs, a is the distance between base pairs, β is the tunneling decay length derived from the tight-binding model, and ν_{tun} is a fitting parameter. The rate for thermal transport is assumed to be

$$\nu_{\text{therm}} \exp\left(-\frac{g_G}{k_B T}\right) \tag{4}$$

where g_G is the energy separation between the hole state on the GC pair and the bottom of the AT band, which is derived from the tight-binding model. There is a critical value of n when these two rates are equal, at which the main mechanism will switch from tunneling to thermal hopping. Using this model, it is estimated to be between three and five, depending on the value of the transfer integral between adjacent base pairs. This is in agreement with the experimental work of Giese et al. [123], where the transfer rate has been found to drop exponentially up to a bridge length of three AT pairs. This also agrees with experimental evidence that suggests some charge is localized on the AT bridge [124, 125]. In this context, the effects of fluctuations and structural distortions have also been considered [86, 173, 175, 196–202].

Long-range charge transfer has also been studied with a scattering matrix formalism and Büttiker's dephasing model [177–181]. The idea behind this approach is that in complex systems, like DNA, charge transfer is unlikely to occur in a single step. Thermal motions of the DNA structure, solvation effects, etc., can break the phase coherence of the charge carrier. The approach thus combines the coherent tunneling and sequential tunneling mechanisms, with relative amount of one to the other determined by the strength of the dephasing. This approach has been successfully employed to account for the experimental results of Porath et al. [135] and Li and Yan [179] on a DNA molecule with 30 GC pairs between two electrodes. A good agreement between experiment and theory has been obtained by assuming partial dephasing.

Using a similar model with two different channels, one for each relative magnetic polarization of the electrodes, Zwolak and Di Ventra [203] predicted that a short poly(dG)–poly(dC) DNA molecule should behave as a spin-valve device; that is, the resistance of the molecule can be changed according to the relative magnetization of the electrodes (see Section 4). Preliminary results from Kasumov seem to confirm that spin-dependent transport can be observed in DNA [204].

Cuniberti et al. [205] used a tight-binding model which includes coupling of the bases to the phosphate backbone to calculate the transport properties of a 30-base pair poly(dG)–poly(dC) DNA between two electrodes. By fitting some parameters in the Hamiltonian, a fairly good agreement between the theoretical and experimental I–V characteristics has been obtained [205]. This result suggests

that the large resistance of the poly(dG)–poly(dC) DNA could be due to the backbone coupling.

Finally, we need to mention that apart from the three main transport mechanisms discussed in this section, polaron [6, 87, 121, 144, 206–212] and soliton [213, 214] formation in DNA have also been investigated. The former relates to the coupling of the electronic and vibrational-mode degrees of freedom, and the latter relates to the formation of domain walls in dimerized bonds of DNA.

Schuster et al. suggested a phonon-assisted, polaronlike hopping mechanism for charge transfer [121, 208]. Since structural fluctuations of DNA are relatively fast [215–217], the local structure around a charged base is likely to rearrange. The distance in between base pairs would thus decrease; the angle between base pairs could also decrease. Other structural changes that trap the charge might occur as well. The resulting polaron could then move through the DNA via temperature-induced structural fluctuations.

Bruinsma et al. suggested, based on a tight-binding model which includes structural fluctuations, a polaronlike hopping mechanism, where the hopping is controlled by structural fluctuations [196]. Charge transfer would then increase strongly with temperature, an effect that is actually observed in some experiments [86, 130]. Barnett et al. put forth an explanation of this temperature dependence which relies on fluctuations in the location of the counterions on the DNA [218]. By performing first-principles calculations, these authors have shown that different counterion configurations can lead to localized hole states. Therefore, fluctuations of the counterions could induce movement of the holes. This would also lead to an increase of the rate of charge transfer with increasing temperature.

Yu and Song [201] explained the temperature dependence observed by Tran et al. [130]. Tran et al. found that the conductivity increases slowly with increasing temperature. However, at high temperatures, the conductivity has been found to be strongly dependent on temperature [130]. This result can be explained by invoking a "variable-range hopping" model with a temperature dependent localization length. Here, the probability of hopping is dependent on two mechanisms, both tunneling (characterized by the localization length) and a thermally activated hopping. Thus, the most probable distance for hopping is due to the competition between these two mechanisms. If this is the case, there is a critical temperature above which the most likely hopping distance becomes smaller than the distance between bases. Above this temperature, the hopping mechanism can only be thermally activated. This fact alone is enough to describe a transition from weak temperature dependence to strong temperature dependence. However, the results from this model do not fit well with experiment [130, 201]. Yu and Song thus calculated the localization length using a tight-binding Hamiltonian which includes fluctuations in the angle between adjacent base pairs. With this correction, the "variable-range hopping" model seems to give the correct temperature dependence.

Hjort and Stafstrom studied charge transfer in poly(dG)–poly(dC) DNA using a tight-binding Hamiltonian [219]. These authors found that including fluctuations of the angle between adjacent base pairs decreases the conductivity of DNA. Likewise, Grozema et al. used a tight-binding Hamiltonian with an electronic coupling that depends on the angle and distance between adjacent base pairs to study the effect of fluctuations [175]. These authors found that the mobility of poly(dG)–poly(dC) DNA decreases by an order of magnitude when structural fluctuations are taken into account. Furthermore, Grozema et al. found that disorder in the site energies of the tight-binding chain, due to, for example, an inhomogeneous distribution of counterions on the DNA, can reduce the mobility by another order of magnitude [175].

4. DNA APPLICATIONS IN NANOSCALE ELECTRONICS

In this section, we discuss the possible application of DNA as an electronic component and its use as a self-assembling template. In the latter case, DNA has been found to aid in the assembly of novel nanoscale structures, which could not be assembled otherwise, and could potentially speed up self-assembly of existing structures.

4.1. DNA Nanoscale Wires

Braun et al. carried out an interesting application of DNA in a rudimentary nanoscale circuit [101, 220]. These authors made a silver wire using DNA as a template [101]. The fabrication method is outlined in Figure 13. Two different

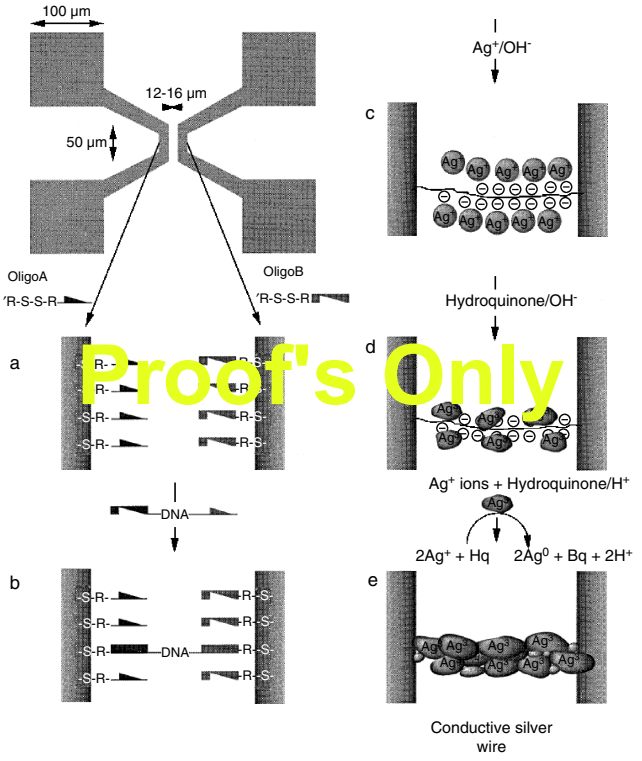

Figure 13. Assembly of a silver wire from a DNA template. (a) The electrodes with attached oligonucleotide groups. (b) A DNA molecule bridging between the two electrodes. (c) Ion exchange of sodium ions with silver ions. (d) Silver deposition onto the DNA. (e) Conductive silver wire. Reprinted with permission from [101], E. Braun et al., *Nature* (*London*) 391, 775 (1998). © 1998, Nature Publishing Group.

12-base oligonucleotides are attached to one of two gold electrodes through a disulphide group at their end. The two electrodes are connected by placing them in a solution of fluorescently labeled λ-DNA. Two 12-base "sticky ends" were added to the λ-DNA. One of these ends hybridized to an electrode. The DNA was then stretched to the other electrode by flow of the solution.

Using an ion-exchange process, Na^+ ions on the DNA backbone are replaced with Ag^+. The silver ions are reduced by a basic hydroquinone solution. Extra silver metal is then deposited by addition of an acidic Ag^+/hydroquinone solution. The resulting silver wire between gold electrodes 12 μm apart is shown in Figure 14. AFM imaging has been used to verify the presence of only a single wire.

The wire, shown in Figure 14, had grains of 30–50 nm continuously placed, and overall had a width of about 100 nm and a length of 12 μm. The size and structure of the wire could be controlled during the different fabrication steps. However, wires with grain sizes of 25 nm or less were found to be discontinuous [101]. The *I–V* characteristics of the silver wire are shown in Figure 15. Its resistance was greater than 10^{13} Ω in the region of low bias. These curves were

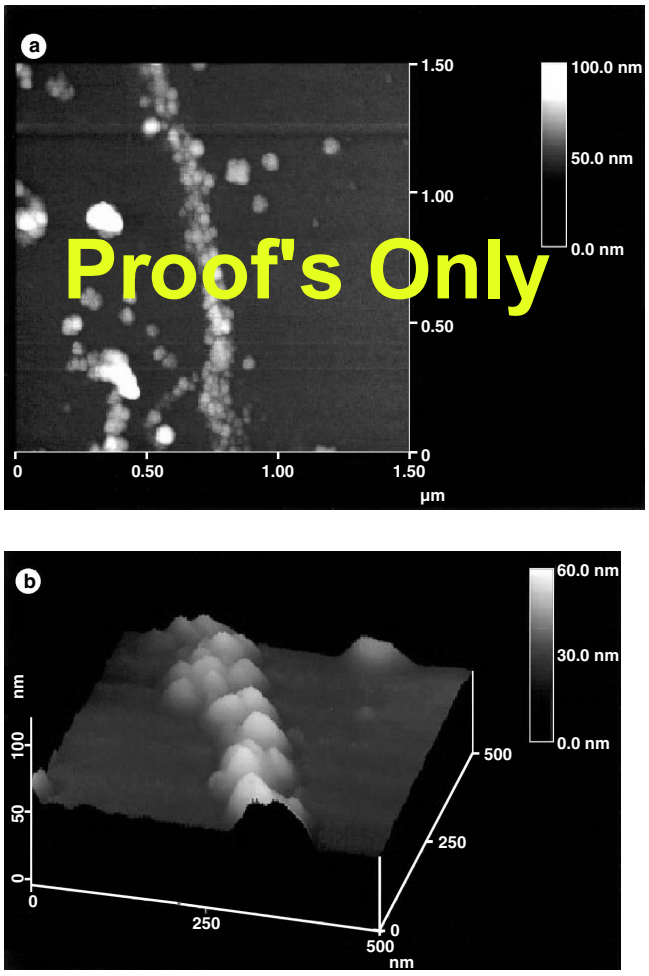

Figure 14. Silver wire fabricated from a DNA template. (a) A 1.5 μm field size image of the silver wire. (b) A 0.5 μm field size image. Reprinted with permission from [101], E. Braun et al., *Nature* (*London*) 391, 775 (1998). © 1998, Nature Publishing Group.

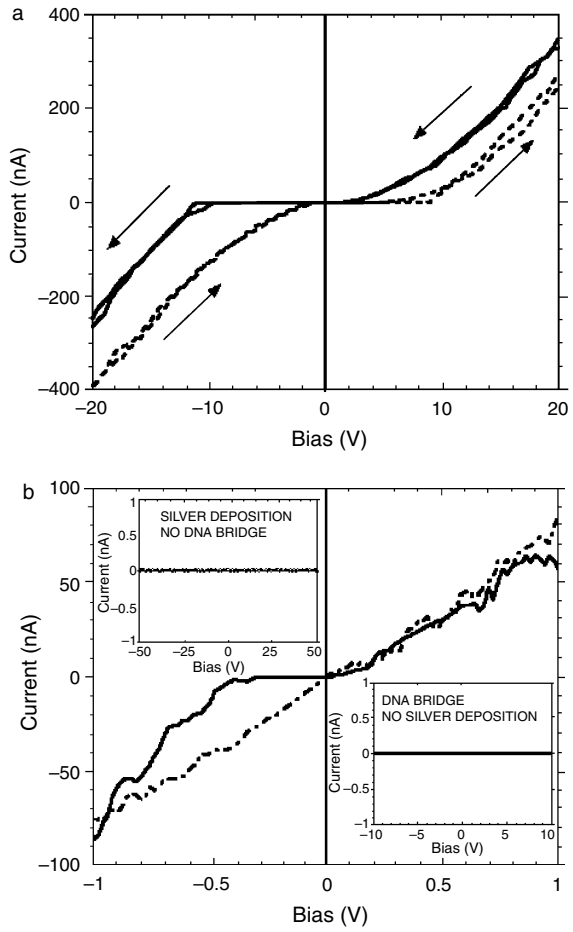

Figure 15. (a) *I–V* characteristics of the 12 μm long and 100 nm wide silver wire. The arrows show the direction of the voltage scan. (b) *I–V* characteristics of a silver wire with more silver deposited. The upper inset shows *I–V* curves with silver deposition and no DNA bridge. The lower inset shows the *I–V* curve with a DNA bridge and no silver deposition. Reprinted with permission from [101], E. Braun et al., *Nature* (*London*) 391, 775 (1998). © 1998, Nature Publishing Group.

reproducible, as shown in Figure 15a, but they showed hysteresis whose origin is still unclear. Figure 15b shows a wire where more silver was deposited. A smaller current gap was found in this case, and the resistance was reduced at higher voltages from 30 to 7 MΩ, showing that the electrical conductivity can be somewhat controlled by silver deposition.

The large current gap in the first case is still unclear. It can be attributed to grain boundary effects or to Coulomb blockade. For practical applications, ohmic behavior is, however, desirable. In this respect, Richter et al. succeeded in making a palladium wire which displayed ohmic behavior [102, 221–223]. A single palladium wire is shown in Figure 16. A drop of λ-DNA solution was placed on gold electrodes. The capillary forces of the evaporating drop aligned the DNA chain between the gold surfaces. A palladium solution was then put on the sample and reduced by addition of a different solution. Finally, the sample was rinsed in order to remove clusters that formed without the DNA. Further addition of palladium solution and reducing agent caused more growth. Like the silver wire, separate metal clusters were observed which eventually become

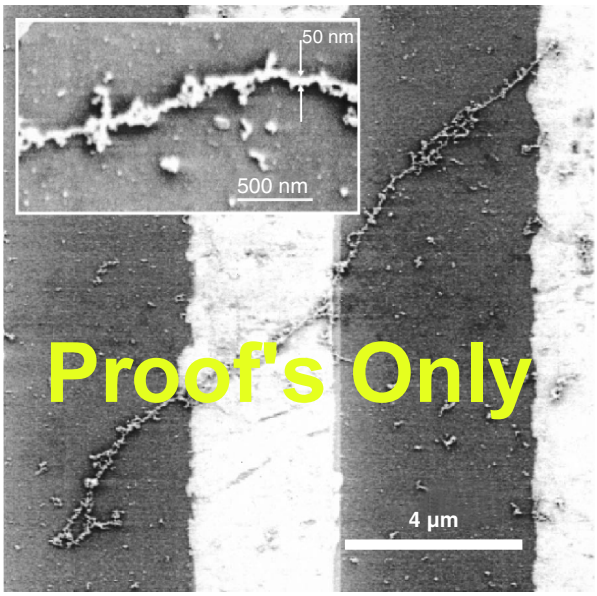

Figure 16. Palladium wire made from metallization of λ-DNA. Reprinted with permission from [102], J. Richter et al., *Appl. Phys. Lett.* 78, 536 (2001). © 2001, American Institute of Physics.

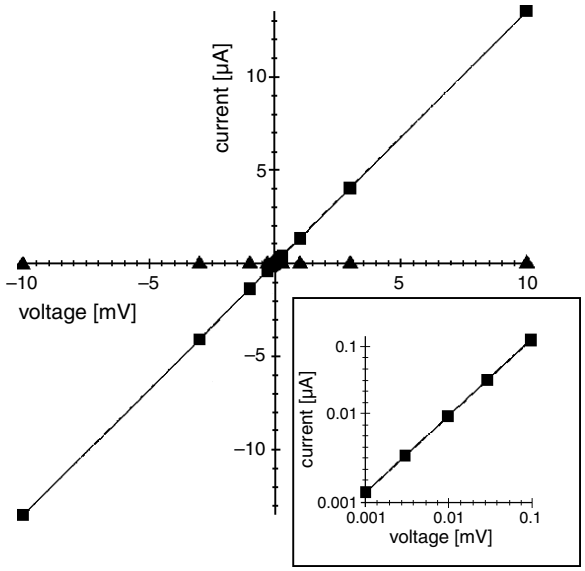

Figure 17. *I–V* characteristics of the palladium wire. Squares correspond to the wire as grown; triangles refer to the wire after it was cut. The inset shows the *I–V* characteristics at low voltages. Reprinted with permission from [102], J. Richter et al., *Appl. Phys. Lett.* 78, 536 (2001). © 2001, American Institute of Physics.

continuous with increased deposition. However, unlike the DNA-template silver wire, the grain sizes were about 3 nm, and the metal clusters aggregated into a continuous structure at about 20 nm of thickness. A linear dependence of the resistance on wire length has also been found [102, 221, 222]. Since none of the wires, including very thick ones, displayed a resistance below ∼5 kΩ, a contact resistance was likely present. This minimum resistance was significantly reduced by "pinning" further wires to the gold electrodes, using electron-beam-induced carbon lines.

Since the fabrication process generates many wires, the resistance of each wire was measured by systematically cutting each one. The resulting wires displayed ohmic behavior (see Fig. 17). The measured resistance was found to be about 700 Ω, which gives a specific conductivity of 2×10^4 S cm^{-1} (i.e., about one order of magnitude less than bulk palladium).

Richter et al. more recently measured the resistance of DNA-templated palladium wires at low temperatures [224]. Above 30 K, the resistance of these wires decreased with decreasing temperature. However, below 30 K, the resistance increased. This type of behavior is observed in two-dimensional 2D disordered metals, like palladium films of similar thickness, where localization occurs due to backscattering without loss of phase coherence of the electrons. The disorder in the palladium wires was attributed to the presence of grain boundaries. In order to decrease the amount of disorder, the DNA-templated palladium wire was annealed. After annealing, the wire no longer showed an increase of resistance at low temperatures, indicating that the resistance increase is indeed due to disorder.

Other groups have also succeeded in fabricating DNA-based nanowires [225–227]. For instance, Harnack et al. made a gold wire network on a DNA template [225]. Gold nanoparticles of 1–2 mm capped with tris(hydroxymethyl)phosphine were bound to DNA [225]. Nanowires as small as 30–40 nm with resistivities about 1000 times larger than bulk gold were fabricated [225]. Ford et al. were able to assemble DNA with 1 nm size platinum grains as a precursor to a larger wire [226]. In this case, the platinum was bound directly to the bases, instead of exploiting the ionic interaction with the backbone. The idea is to be able to create smaller wires with the desired *I–V* characteristics [223, 226, 228].

Kumar et al. exploited the electrostatic interactions with the DNA backbone to create linear arrays of nanoparticles, which could potentially be used to create an array of wires [229]. Lysine-capped, ∼3 nm colloidal gold particles were mixed with DNA. The DNA–gold hybrids were separated out after the solution sat for two hours. The experiment was carried out with two types of synthetic DNA and calf-thymus DNA. Figure 18A shows the transmission electron microscopy (TEM) image of a 15-base pair, synthetic DNA–gold hybrid on a carbon coated TEM grid. The linear arrays of gold nanoparticles can clearly be seen in the image. The separation of the arrays is about 9 nm. Figure 18B shows the scanning tunneling microscopy (STM) image of the 30-base pair synthetic DNA–gold hybrid on a silicon wafer. However, the electrical properties of these structures have not been measured, so no conclusion can be drawn about their conducting properties. Sastry et al. created DNA–gold hybrids using similar methods [230].

Another way of fabricating nanowires is to use M-DNA [231–233]. In M-DNA, the imino proton (a proton attached to a nitrogen which is double-bonded to a carbon) is replaced by a divalent metal atom, like Zn^{2+}, Co^{2+}, and Ni^{2+} [233]. B-DNA together with one of those ions will form M-DNA in a solution with a pH larger than 8. The metal ion not only alters the electronic structure of DNA but also its physical structure. The base pair separation is about 4 Å

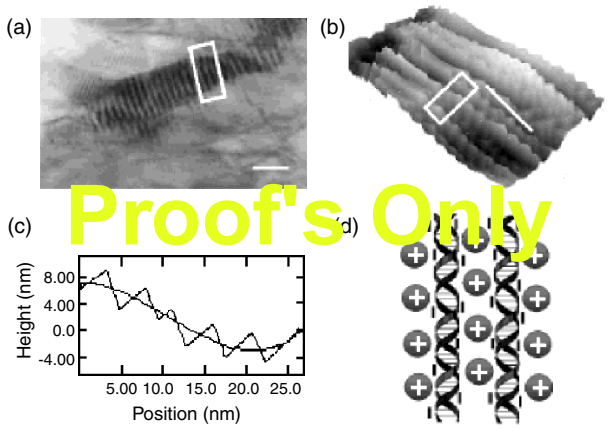

Figure 18. (A) TEM image of a 15-base pair synthetic DNA–gold hybrid on a carbon coated TEM grid. (B) STM image of the 30-base pair synthetic DNA–gold hybrid on a silicon wafer. (C) Height versus distance along the line shown in (B). (D) Schematic of the DNA–gold hybrid. Reprinted with permission from [229], A. Kumar et al., *Adv. Mater.* 13, 341 (2001). © 2001, Wiley–VCH.

in M-DNA compared to 3.4 Å in B-DNA. Figure 19 shows the base pairs in M(Zn)-DNA.

To measure the *I–V* characteristics, a DNA chain was placed across a deep gap, which kept salt bridges from forming and guaranteed that the DNA chain was the only conducting element of the device [231]. This was done by placing a drop of either B-DNA or M-DNA across the electrodes. The corresponding current–voltage characteristics in vacuum and at room temperature were measured. The B-DNA displayed semiconducting behavior, with a current gap of about 200 meV. The M-DNA, however, showed no gap but comparable behavior at higher biases. The lack of a current gap was attributed to the zinc ions bringing the edge of the DNA molecular bands closer to the Fermi level of the gold electrodes. As in the experiment of Braun et al. [101], transport through B-DNA with "sticky ends" has also been measured. In this case, large-bandgap semiconducting behavior was observed in B-DNA, reminiscent of the behavior found by Porath et al. [135]. The presence of this large current gap was attributed to the end groups limiting the current.

The same group finds that electron transfer is greatly enhanced in M-DNA compared to B-DNA from fluorescence quenching measurements [232, 234, 235]. Most recently, significant quenching at distances up to ~150 nm has been reported [232, 234, 235]. Weak distance dependence suggests that electron hopping is the main mechanism for transport in M-DNA.

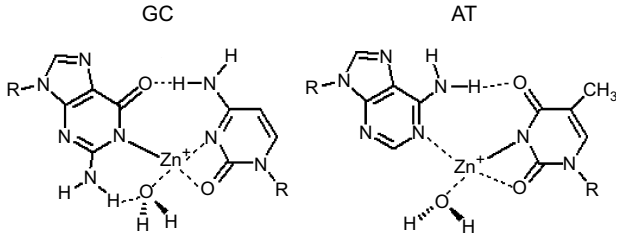

Figure 19. Base pairs in M-DNA, with Zn^{2+} as the metal ion.

Zwolak and Di Ventra recently suggested that short DNA wires can be used as spin valve devices [203]. A short poly(dG)–poly(dC) between two magnetic electrodes was studied as an example. By assuming negligible spin-flip scattering in the wire and at the contacts, magnetoresistance values of as much as 26% for Ni and 16% for Fe contacts were predicted. The magnetoresistance is defined as $(R_{\text{anti}} - R_{\text{parallel}})/R_{\text{anti}}$, where R is the resistance for each relative magnetization of the electrodes. The calculated magnetoresistance is shown in Figure 20. Kasumov recently performed experiments with DNA between permalloy electrodes [204] and actually observed spin-dependent transport in DNA.

Finally, Ben-Jacob et al. suggested, based on the idea that each phosphate group can act as a tunnel junction, that DNA could be used as a transistor or even as a quantum bit [214, 236].

4.2. DNA Self-Assembly

The different properties of DNA make it particularly versatile in several applications from computation to fueling nanomechanical devices [237–250]. In addition, DNA's recognition ability has been found to help in the self-assembly of novel nanoscale structures out of "nanoscale building blocks" (e.g., nanoparticles) [103, 251–255]. In this section, we will review the research done on assembling large-scale structures relevant to nanoscale electronics using DNA.

Ordering of nanoparticles is important to realize electronic devices and storage media. However, it is a difficult task, for instance, to order hexagonal closed-packed structures [256–260]. A DNA template, on the other hand, is flexible enough that it can be shaped in many different ways. For example, several geometrical structures of DNA have already been made, such as cubes and knots [261]. Periodic arrays are being examined as the main components in nanoscale memory devices and other electronic applications. One potential downfall of using DNA in these applications is that the resulting structures are not rigid [261]. However, this problem can be overcome by assembly onto surfaces (see, e.g., [262–265]). Before discussing different nanoparticle

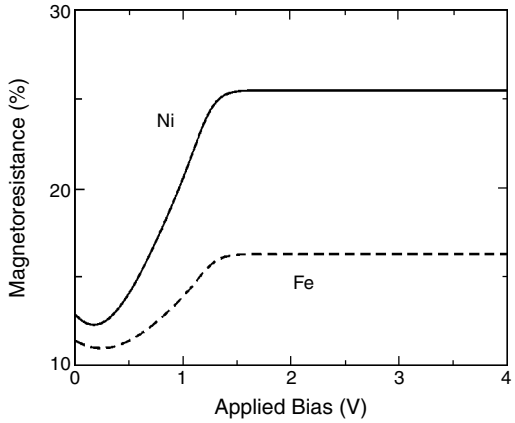

Figure 20. Theoretical magnetoresistance for 30-base pair poly(dG)–poly(dC) DNA between nickel and iron electrodes as a function of bias. Reprinted with permission from [203], M. Zwolak and M. Di Ventra, *Appl. Phys. Lett.* 81, 925 (2002). © 2001, American Institute of Physics.

structures, we review some recent work on molecular lithography (i.e., the patterning of functional devices) using DNA.

Keren et al. demonstrated molecular lithography using DNA [266]. The suggested process starts with a polymerization of RecA protein monomers with a single strand of DNA. The RecA protein mediates homologous recombination between the single strand of DNA and a double strand of DNA. Homologous recombination binds the single stranded DNA to the double-stranded DNA with an identical sequence. Thus, the sequence of the single strand of DNA will determine where it is "placed" on the double strand of DNA. As a consequence, the new double strand of DNA has a section which has the RecA protein bound to it. This section is not coated with metal in the process that will be described. A gold wire was fabricated on the DNA template as follows. The new double strand of DNA was stretched across a passivated silicon surface and then incubated in an $AgNO_3$ solution. The original double strand of DNA had aldehyde bound to it. The aldehyde allowed for small silver aggregates to form on the DNA. The DNA was then further metallized by electroless deposition of gold on top of the silver. This process produced a piece of DNA wire on an insulating surface, which had an insulating gap on the portion where the RecA was bound. It was found that the conductivity of a 50–100 nm thick gold wire, using the aforementioned process, was only about one-seventh that of bulk gold.

Small particles can also be attached to the RecA bound length. A single strand of biotin-labeled DNA binds specifically to the length of DNA that is bound to the RecA. It remains bound even after the protein is removed. This product, then, was used to specifically bind streptavidin-conjugated gold nanoparticles, which attach only to biotin-labeled DNA. After further gold deposition, a piece of metallized DNA formed between two sections of DNA.

Using a similar process, Keren et al. were also able to fabricate a gold cluster [266]. This was done by reacting the primary antibodies of RecA with the DNA that had the RecA bound length. Then secondary antibodies were used with conjugated gold particles. The latter bind to the antibodies. After further gold deposition, the result was a piece of DNA with a localized metal cluster. In addition, by using two double strands of DNA, Keren et al. were able to demonstrate the ability of RecA to create a three-arm junction at a specific location on the DNA. This work demonstrated the potential of DNA to integrate devices on the molecular scale and to create novel functional devices.

Other researchers have focused on the organization of nanoparticles [251, 252, 267, 268]. Although no specific device/structure has been created for use in molecular electronics, this research area shows tremendous potential. Alivisatos et al., for instance, have attached single-stranded DNA to gold nanoparticles. The latter self-assemble onto a complementary DNA template [252]. This approach can form complex structures. Using a similar strategy, Mbindyo et al. attached gold wires to a gold surface [267]. In these structures, single-stranded DNA was attached to specific sites of gold wires 200 nm in diameter. These strands of DNA were complementary to strands on a gold surface.

Other strategies have also been used to attach nanoparticles to surfaces [269]. As an example, Coffer et al. used DNA as a template for the formation of CdS nanoparticles [265, 270–272]. Cd^{2+} ions were added to a solution of plasmid DNA, which formed a DNA/Cd^{2+} complex via electrostatic interaction with the DNA backbone. The DNA was then bound to a solid surface. An array of CdS nanoparticles formed along the DNA upon addition of H_2S. The resulting nanoparticles were relatively monodisperse. Further study has shown that the particular sequence affects the size of the particles [271].

The use of streptavidin–biotin interactions has also been suggested to create arrays of nanoparticles and molecules [273–275]. Winfree et al. used double crossover DNA (i.e., two double-stranded DNA chains which are linked twice by a crossover junction) to create two-dimensional DNA crystals [237]. These methods were shown to be useful in the creation of regular structures.

Mirkin et al. [251] and Alivisatos et al. [252] were among the first to link nanoparticles together using DNA. Mirkin et al. attached two different oligonucleotides to different 13 nm gold particles using a thiol group [251]. Upon addition of a duplex DNA with two "sticky ends," each complementary to one of the oligonucleotides, the gold particles were networked together. Mirkin et al. found the formation of ordered 2D networks of the gold particles. If heated above the dissociation temperature of the DNA duplex, the process could be reversed. This method allows for the assembly of structures with a wide range of parameters (e.g., nanoparticle spacing, size, and composition) [276–278]. Park et al. measured the conductivity of these gold nanoparticle networks [279] and found semiconducting behavior regardless of the length of the DNA linker. This was attributed to collapse of the network upon drying. Mucic et al. even assembled binary networks of gold nanoparticles with two different sizes [276]. A similar method to those just described was extended to other types of nanoparticles as well [277].

Alivisatos et al. assembled 1.4 nm gold particles with one *N*-propylmaleimide attached [252]. This maleimido group could be coupled to a sulphydryl group on an oligonucleotide. Adding a single-stranded DNA as a template, these oligonucleotide substituents formed the corresponding duplex DNA. With this method, Alivisatos et al. were able to create well spaced gold particles along the DNA template.

Niemeyer et al. used streptavidin as a model particle to which only a few biotinylated DNA molecules can bind [280]. These researchers found that by changing the ionic conditions, the streptavidin–DNA network changes. Under ionic conditions, double-stranded DNA condensed into supercoils (i.e., the double helix axis is itself twisted). This caused the contour length of the DNA to decrease, thereby bringing bound streptavidin closer together, hence changing the topology of the networks. Transition in the structure of DNA is a mechanism behind nanomechanical devices based on DNA [243, 244, 249].

Dwyer et al. functionalized carbon nanotubes with DNA [281]. Open-ended, single-walled carbon nanotubes with terminal carboxylic acid groups were reacted with amino-terminated DNA strands. This reaction covalently attached the DNA to the nanotube. Exploiting DNA's self-assembly properties, these functionalized nanotubes could be assembled onto surfaces or into structured networks.

Another approach to build functional devices has relied on the modification of semiconductor surfaces with DNA. These modified surfaces can then be used to fabricate nanoscale electronic devices [282, 283]. Pike et al., for instance, used photolithography and anodic etching on a silicon surface with a carbon monolayer to attach double-stranded DNA in an organized manner [282]. However, a good electrical contact between the DNA and the surface has yet to be established.

Demers et al. used "dip-pen nanolithography" to pattern DNA on a gold surface and on a silicon oxide surface [284]. Dip-pen nanolithography consists of a silanized AFM tip, which is dipped into a "DNA ink" (i.e., a solution of 90% dimethyl-formamide/10% water containing 1 mM DNA and 0.3 M $MgCl_2$). The "AFM pen" is then used to directly "write" the DNA onto the surfaces. The DNA used consisted of hexanethiol-modified oligonucleotides. In one case, dip-pen nanolithography was used to "write" DNA onto a gold surface, where the thiol group adsorbs onto the surface [284]. The surface was then placed into a solution containing an alkane-thiol, which protects the surface from adsorption of other elements, (e.g., nanoparticles). The DNA-patterned gold surface was then used to assemble DNA modified gold nanoparticles. One benefit of this method is the ability to write patterns on the surface with different oligonucleotides, which can then be used to assemble more complicated structures. Another benefit is the ability to vary the feature size by varying the experimental conditions while writing to the surface. A change in humidity of 15% was found to change the size of the DNA spot six times [284]. Demers et al. also used this method to pattern DNA on a silicon oxide surface [284]. Here, an oxidized silicon wafer was activated by treatment with 3′-mercaptopropyltrimethoxysilane. The DNA in the "DNA ink" was an oligonucleotide modified with an acrylamide group, which reacts with the silane on the silicon surface. Finally, protection of the rest of the silicon surface was done by reaction with acrylic acid.

We conclude this section by noting that although functional nanoparticle networks for nanoscale electronics have yet to be demonstrated using DNA assembly, rapid progress in this area suggests that such goal is not so difficult to achieve. For instance, an aspect of this research that has yet to be developed, but which shows great potential for applications, is the assembly of magnetic nanoparticles using DNA. Assembling nanoparticles with coercivity large enough to maintain their magnetization at room temperature would constitute a considerable advancement in creating self-assembled nanoscale memory devices.

5. CONCLUSIONS

We have reviewed the transport properties of DNA with particular emphasis on its possible use in nanoscale electronics. DNA shows a large number of conducting properties due the large phase space in which it can be made and assembled. The physical interpretation of these properties is not completely clear yet. Notwithstanding this, DNA is already occupying an important place in nanoscale science due to its self-assembly and recognition properties. The different functional properties of this important biological molecule promise to find practical use in many electronic applications that have yet to be completely explored at the nanoscale.

GLOSSARY

DNA Deoxyribonucleic acid. DNA is a macromolecule made of four different monomers. Each monomer unit, called a nucleotide, consists of a phosphate group, a five-carbon sugar, and one of four bases.

Fluorescence The emission of light by a substance immediately after the absorption of energy from light of usually shorter wavelength.

Molecular lithography The use of information stored in a molecular structure to direct the formation of a patterned structure at the nanoscale.

Self-assembly Coordination of several entities to form a larger structure (e.g., the coordination of molecules and a gold surface to form a layer of molecules on that surface).

Sequential tunneling A mechanism of charge transport through a series of energy barriers. Each barrier is transversed by tunneling, and the charge carrier is localized before it transverses the next barrier.

Thermal hopping A mechanism of charge transport which relies on thermal excitation of charge carriers to give them the required energy to transverse an energy barrier.

Tunneling A mechanism of charge transport which relies on the quantum mechanical nature of charge carriers that allows particles to transverse an energy barrier at a lower energy than the barrier itself.

ACKNOWLEDGMENTS

We thank A. Yu. Kasumov for communicating his results on surface-induced DNA compression and spin-dependent transport prior to publication. The authors acknowledge partial support from the National Science Foundation grants DMR-01-02277 and DMR-01-33075 and the Carilion Biomedical Institute. Acknowledgment is also made to the Donors of The Petroleum Research Fund, administered by the American Chemical Society, for partial support of this research.

REFERENCES

1. J. D. Watson and F. H. C. Crick, *Nature* (*London*) 171, 737 (1953).
2. S. Steenken, *Chem. Rev.* 89, 503 (1989).
3. E. D. A. Stemp, M. R. Arkin, and J. K. Barton, *J. Am. Chem. Soc.* 119, 2921 (1997).
4. D. B. Hall and J. K. Barton, *J. Am. Chem. Soc.* 119, 5045 (1997).
5. M. R. Arkin, E. D. A. Stemp, S. C. Pulver, and J. K. Barton, *Chem. Biol.* 4, 389 (1997).
6. D. T. Breslin, J. E. Coury, J. R. Anderson, L. McFail-Isom, Y. Kan, L. D. Williams, L. A. Bottomley, and G. B. Schuster, *J. Am. Chem. Soc.* 119, 5043 (1997).
7. W. Chen, C. Turro, L. A. Friedman, J. K. Barton, and N. J. Turro, *J. Phys. Chem. B* 101, 6995 (1997).
8. B. Demple and L. Harrison, *Annu. Rev. Biochem.* 63, 915 (1994).
9. S. Loft and H. E. Poulsen, *J. Mol. Med.* 74, 297 (1996).
10. V. Guallar, A. Douhal, M. Moreno, and J. M. Lluch, *J. Phys. Chem. A* 103, 6251 (1999).

11. S. Steenken, *Biol. Chem.* 378, 1293 (1997).
12. H. L. Chen and P. Yang, *Progr. Chem.* 14, 239 (2002).
13. A. Heller, *Faraday Discuss.* 116, 1 (2000).
14. D. R. Meldrum and M. R. Holl, *Science* 297, 1197 (2002).
15. T. A. Taton, C. A. Mirkin, and R. L. Letsinger, *Science* 289, 1757 (2000).
16. C. V. Kumar, E. H. A. Punzalan, and W. B. Tan, *Tetrahedron* 56, 7027 (2000).
17. J. J. Kasianowicz, E. Brandin, D. Branton, and D. W. Deamer, *Proc. Nat. Acad. Sci. USA* 93, 13770 (1996).
18. W. Vercoutere, S. Winters-Hilt, H. Olsen, D. Deamer, D. Haussler, and M. Akeson, *Nature Biotechnol.* 19, 258 (2001).
19. J. Li, D. Stein, C. McMullan, D. Branton, M. J. Aziz, and J. A. Golovchenko, *Nature* (*London*) 412, 166 (2001).
20. A. Meller, L. Nivon, and D. Branton, *Phys. Rev. Lett.* 86, 3435 (2001).
21. R. H. Terbrueggen, T. W. Johann, and J. K. Barton, *Inorg. Chem.* 37, 6874 (1998).
22. T. W. Johann and J. K. Barton, *Philos. Trans. Roy. Soc. London Ser. A* 354, 299 (1996).
23. D. Wemmer, *Annu. Rev. Biophys. Biomol. Struct.* 29, 439 (2000).
24. D. Wemmer, *Nat. Struct. Biol.* 5, 169 (1998).
25. A. Marziali and M. A. Akeson, *Annu. Rev. Biomed. Eng.* 3, 195 (2001).
26. A. Marshall and J. Hodgson, *Nature Biotechnol.* 16, 27 (1998).
27. S. O. Kelley, N. M. Jackson, M. G. Hill, and J. K. Barton, *Angew. Chem., Int. Ed.* 38, 941 (1999).
28. F. Lisdat, B. Ge, and F. W. Scheller, *Electrochem. Commun.* 1, 65 (1999).
29. F. Lisdat, B. Ge, B. Krause, A. Ehrlich, H. Bienert, and F. W. Scheller, *Electroanal.* 13, 1225 (2001).
30. J. J. Gooding, *Electroanal.* 14, 1149 (2002).
31. S. Kumamoto, H. Nakano, Y. Matsuo, Y. Sugie, and K. Yamana, *Electrochemistry* 70, 789 (2002).
32. E. M. Boon, J. K. Barton, P. I. Pradeepkumar, J. Isaksson, C. Petit, and J. Chattopadhyaya, *Angew. Chem., Int. Ed.* 41, 3402 (2002).
33. A. Erdem and M. Ozsoz, *Electroanal.* 14, 965 (2002).
34. R. P. Fahlman and D. Sen, *J. Am. Chem. Soc.* 124, 4610 (2002).
35. M. J. Heller, *Annu. Rev. Biomed. Eng.* 4, 129 (2002).
36. C. Dekker and M. A. Ratner, *Phys. World* 14, 29 (2001).
37. S. F. Nelson, Y.-Y. Lin, D. J. Gundlach, and T. N. Jackson, *Appl. Phys. Lett.* 72, 1854 (1998).
38. W. A. Schoonveld, J. Vrijmoeth, and T. M. Klapwijk, *Appl. Phys. Lett.* 73, 3884 (1998).
39. A. M. van de Craats, L. D. A. Siebbeles, I. Bleyl, D. Haarer, Y. A. Berlin, A. A. Zharikov, and J. M. Warman, *J. Phys. Chem. B* 102, 9625 (1998).
40. H. McConnel, *J. Chem. Phys.* 35, 508 (1961).
41. D. D. Eley and D. I. Spivey, *Trans. Faraday Soc.* 58, 411 (1962).
42. R. S. Snart, *Trans. Faraday Soc.* 59, 754 (1963).
43. H. Pohl and W. Kauzman, *Rev. Mod. Phys.* 36, 721 (1963).
44. T. A. Hoffmann and J. Ladik, *Advan. Chem. Phys.* 7, 84 (1964).
45. C. T. O'Konski, P. Moser, and M. Shirai, *Biopolymers*, Symp. No. 1, 479 (1964).
46. R. S. Snart, *Biopolymers* 6, 293 (1968).
47. B. B. Singh, *Adv. Med. Phys.* 12, 245 (1968).
48. J. Ladik, *Int. J. Quant. Chem.* 3S, 307 (1971).
49. S. Suhai, *J. Chem. Phys.* 57, 5599 (1972).
50. M. F. Lecompte, D. Muller, and M. Josefowicz, *Biopolymers* 11, 2563 (1972).
51. D. Dee and M. E. Baur, *J. Chem. Phys.* 60, 541 (1974).
52. R. Pethig, "Dielectric and Electronic Properties of Biological Materials." Wiley, New York, 1979.
53. B. C. Baguley and M. Lebret, *Biochemistry* 23, 937 (1984).
54. C. V. Kumar, J. K. Barton, and N. J. Turro, *J. Am. Chem. Soc.* 107, 5518 (1985).
55. P. Fromherz and B. Rieger, *J. Am. Chem. Soc.* 108, 5361 (1986).
56. J. K. Barton, C. V. Kumar, and N. J. Turro, *J. Am. Chem. Soc.* 108, 6391 (1986).
57. J. D. Magan, W. Blau, D. T. Croke, D. J. McConnell, and J. M. Kelley, *Chem. Phys. Lett.* 141, 489 (1987).
58. D. D. Eley, *Mol. Cryst. Liquid Cryst.* 171, 1 (1989).
59. A. M. Brun and A. Harriman, *J. Am. Chem. Soc.* 114, 3656 (1992).
60. Y. Lee, H. H. Heasley, J. A. Thompson, K. Murata, B. M. Hoffman, T. M. Haard, P. J. Hamot, W. P. Halperin, and P. Wölfle, *Europhys. Lett.* 36, 681 (1996).
61. A. M. van de Craats, J. M. Warman, M. P. de Haas, D. Adam, J. Simmerer, D. Haarer, and P. Schuhmacher, *Adv. Mater.* 8, 823 (1996).
62. A. M. van de Craats, P. G. Schouten, and J. M. Warman, *Ekisho* 2, 12 (1998).
63. A. M. van de Craats and J. M. Warman, *Adv. Mater.* 13, 130 (2001).
64. P. G. Schouten, J. M. Warman, M. P. de Haas, M. A. Fox, and H. L. Pan, *Nature* (*London*) 353, 736 (1991).
65. P. G. Schouten, J. M. Warman, M. P. de Haas, J. F. van der Pol, and J. W. Zwikker, *J. Am. Chem. Soc.* 114, 9028 (1992).
66. C. J. Murphy, M. R. Arkin, Y. Jenkins, N. D. Ghatlia, S. H. Bossmann, N. J. Turro, and J. K. Barton, *Science* 262, 1025 (1993).
67. Y. Okahata, T. Kobayashi, K. Tanaka, and M. Shimomura, *J. Am. Chem. Soc.* 120, 6165 (1998).
68. C. J. Burrows and J. G. Muller, *Chem. Rev.* 98, 1109 (1998).
69. J. Cadet, in "DNA Adducts: Identification and Significance" (K. Hemminki, A. Dipple, D. E. F. Shiker, F. F. Kadlubar, D. Segerback, and H. Bartsch, Eds.). IARC, Lyon, France, 1994.
70. M. R. Arkin, E. D. A. Stemp, R. E. Holmlin, J. K. Barton, A. Hörmann, E. J. C. Olson, and P. F. Barbara, *Science* 273, 475 (1996).
71. S. O. Kelley and J. K. Barton, *Science* 273, 475 (1996).
72. T. J. Meade and J. F. Kayyem, *Angew. Chem. Int. Ed. Engl.* 34, 352 (1995).
73. F. D. Lewis, T. Wu, Y. Zhang, R. L. Letsinger, S. R. Greenfield, and M. R. Wasielewski, *Science* 277, 673 (1997).
74. S. O. Kelley, R. E. Holmlin, E. D. A. Stemp, and J. K. Barton, *J. Am. Chem. Soc.* 119, 9861 (1997).
75. E. Meggers, M. E. Michel-Beyerle, and B. Giese, *J. Am. Chem. Soc.* 120, 12950 (1998).
76. S. O. Kelley and J. K. Barton, *Chem. Biol.* 5, 413 (1998).
77. K. Fukui and K. Tanaka, *Angew. Chem. Int. Ed. Engl.* 37, 158 (1998).
78. S. O. Kelley and J. K. Barton, *Science* 283, 375 (1999).
79. S. Priyadarshy, S. M. Risser, and D. N. Beratan, *J. Phys. Chem.* 100, 17678 (1996).
80. A. K. Felts, W. T. Pollard, and R. A. Friesner, *J. Phys. Chem.* 99, 2929 (1995).
81. A. Okada, V. Chernyak, and S. Mukamel, *J. Phys. Chem. A* 102, 1241 (1998).
82. T. L. Netzel, in "Organic and Inorganic Photochemistry" (V. Ramamurthy and K. S. Schanze, Eds.), pp. 1–54. Dekker, New York, 1998.
83. M. Ratner, *Nature* (*London*) 397, 480 (1999).
84. P. J. Dandliker, R. E. Holmlin, and J. K. Barton, *Science* 275, 1465 (1997).
85. D. B. Hall, R. E. Holmlin, and J. K. Barton, *Nature* (*London*) 382, 731 (1996).
86. C. Wan, T. Fiebig, S. O. Kelley, C. R. Treadway, J. K. Barton, and A. H. Zewail, *Proc. Natl. Acad. Sci. USA* 96, 6014 (1999).
87. S. M. Gasper and G. B. Schuster, *J. Am. Chem. Soc.* 119, 12762 (1997).
88. G. Taubes, *Science* 275, 1420 (1997).
89. J. M. Warman, M. P. de Haas, and A. Rupprecht, *Chem. Phys. Lett.* 249, 319 (1996).
90. T. Fiebig, C. Wan, S. O. Kelley, J. K. Barton, and A. H. Zewail, *Proc. Natl. Acad. Sci. USA* 96, 1187 (1999).
91. C. Wan, T. Fiebig, O. Schiemann, J. K. Barton, and A. H. Zewail, *Proc. Natl. Acad. Sci. USA* 97, 14052 (1999).

92. Y. Okahata, T. Kobayashi, H. Nakayama, and K. Tanaka, *Supramol. Sci.* 5, 317 (1998).
93. D. Dunlap, R. Garcia, E. Schabtach, C. Bustamante, *Proc. Natl. Acad. Sci. USA* 90, 7652 (1993).
94. R. Guckenberger, M. Heim, G. Cevc, H. F. Knapp, W. Wiegrabe, and A. Hillebrand, *Science* 266, 1538 (1994).
95. R. P. Fahlman, R. D. Charma, and D. Sen, *J. Am. Chem. Soc.* 124, 12477 (2002).
96. S. Priyadarshy, S. M. Risser, and D. N. Beratan, *J. Biol. Inorg. Chem.* 3, 196 (1998).
97. N. J. Turro and J. K. Barton, *J. Biol. Inorg. Chem.* 3, 201 (1998).
98. T. L. Netzel, *J. Biol. Inorg. Chem.* 3, 210 (1998).
99. F. D. Lewis and R. L. Letsinger, *J. Biol. Inorg. Chem.* 3, 215 (1998).
100. E. S. Krider and T. J. Meade, *J. Biol. Inorg. Chem.* 3, 222 (1998).
101. E. Braun, Y. Eichen, U. Sivan, and G. Ben-Yoseph, *Nature* (*London*) 391, 775 (1998).
102. J. Richter, M. Mertig, W. Pompe, I. Monch, and H. K. Schackert, *Appl. Phys. Lett.* 78, 536 (2001).
103. J. J. Storhoff and C. A. Mirkin, *Chem. Rev.* 99, 1849 (1999).
104. P. S. Weiss, *Nature* (*London*) 413, 585 (2001).
105. T. Yokoyama, S. Yokoyama, T. Kamikado, Y. Okuno, and S. Mashiko, *Nature* (*London*) 413, 619 (2001).
106. C. M. Niemeyer, *Curr. Opin. Chem. Biol.* 4, 609 (2000).
107. C. M. Niemeyer, *Angew. Chem., Int. Ed.* 40, 4128 (2001).
108. S. Mann, *Nature* (*London*) 365, 499 (1993).
109. W. Shenton, S. A. Davis, and S. Mann, *Adv. Mater.* 11, 449 (1999).
110. R. Kirsch, M. Mertig, W. Pompe, R. Wahl, G. Sadowski, K. J. Bohm, and E. Unger, *Thin Solid Films* 305, 248 (1997).
111. M. Mertig, R. Kirsch, W. Pompe, and H. Engelhardt, *Eur. Phys. J. D* 9, 45 (1999).
112. R. Wahl, M. Mertig, W. Pompe, S. Selenska-Pobell, and J. Raffi, *Adv. Mater.* 13, 736 (2001).
113. U. B. Sleytr, M. Sara, D. Pum, and B. Schuster, *Progr. Surf. Sci.* 68, 231 (2001).
114. S.-W. Lee, C. Mao, C. E. Flynn, and A. M. Belcher, *Science* 296, 892 (2002).
115. A. M. Brun and A. Harriman, *J. Am. Chem. Soc.* 116, 10383 (1994).
116. A. Harriman, *Angew. Chem. Int. Ed.* 38, 945 (1999).
117. P. Lincoln, E. Tuite, and B. Norden, *J. Am. Chem. Soc.* 119, 1454 (1997).
118. E. J. C. Olson, D. Hu, A. Hörmann, and P. F. Barbara, *J. Phys. Chem. B* 101, 299 (1997).
119. B. Giese, *Annu. Rev. Biochem.* 71, 51 (2002).
120. E. M. Boon and J. K. Barton, *Curr. Opin. Struc. Biol.* 12, 320 (2002).
121. P. T. Henderson, D. Jones, G. Hampikian, Y. Kan, and G. B. Schuster, *Proc. Nat. Acad. Sci. USA* 96, 8353 (1999).
122. A. A. Voityuk, J. Jortner, M. Bixon, and N. Rosch, *Chem. Phys. Lett.* 324, 430 (2000).
123. B. Giese, J. Amaudrut, A.-K. Kohler, M. Spormann, and S. Wessely, *Nature* (*London*) 412, 318 (2001).
124. T. T. Williams, D. T. Odom, and J. K. Barton, *J. Am. Chem. Soc.* 122, 9048 (2000).
125. V. Sartor, E. Boone, and G. B. Schuster, *J. Phys. Chem. B* 105, 11057 (2001).
126. C. Gómez-Navarro, A. Gil, M. Álvarez, P. J. de Pablo, F. Moreno-Herrero, I. Horcas, R. Fernańdez-Sánchez, J. Colchero, J. Gómez Herrero, and A. M. Baró, *Nanotechnology* 13, 314 (2002).
127. A. Gil, P. J. de Pablo, J. Colchero, J. Gómez Herrero, and A. M. Baró, *Nanotechnology* 13, 309 (2002).
128. C. Gómez-Navarro, F. Moreno-Herrero, P. J. de Pablo, J. Colchero, J. Gómez Herrero, and A. M. Baró, *Proc. Nat. Acad. Sci. USA* 99, 8484 (2002).
129. M. Bockrath, N. Markovic, A. Shepard, M. Tinkham, L. Gurevich, L. P. Kouwenhoven, M. W. Wu, and L. L. Sohn, *Nano Lett.* 2, 187 (2002).
130. P. Tran, B. Alavi, and G. Gruner, *Phys. Rev. Lett.* 85, 1564 (2000).
131. H.-W. Fink and C. Schonenberger, *Nature* (*London*) 398, 407 (1999).
132. H.-W. Fink, *Cell. Mol. Life Sci.* 58, 1 (2001).
133. H.-W. Fink, H. Schmid, E. Ermantraut, and T. Schulz, *J. Opt. Soc. Am. A* 14, 2168 (1997).
134. P. J. de Pablo, F. Moreno-Herrero, J. Colchero, J. Gómez Herrero, P. Herrero, A. M. Baró, P. Ordejón, J. M. Soler, and E. Artacho, *Phys. Rev. Lett.* 85, 4992 (2000).
135. D. Porath, A. Bezryadin, S. de Vries, and C. Dekker, *Nature* (*London*) 403, 635 (2000).
136. A. Bezryadin and C. Dekker, *J. Vac. Sci. Technol. B* 15, 793 (1997).
137. A. Bezryadin, C. Dekker, and G. Schmid, *Appl. Phys. Lett.* 71, 1273 (1997).
138. H. Watanabe, C. Manabe, T. Shigematsu, K. Shimotani, and M. Shimizu, *Appl. Phys. Lett.* 79, 2462 (2001).
139. J. S. Hwang, G. S. Lee, K. J. Kong, D. J. Ahn, S. W. Hwang, and D. Ahn, *Microelectron. Eng.* 63, 161 (2002).
140. J. S. Hwang, G. S. Lee, D. Ahn, G. S. Lee, D. J. Ahn, and S. W. Hwang, *Appl. Phys. Lett.* 81, 1134 (2002).
141. A. Yu. Kasumov and D. V. Klinov, private communication.
142. T. Muir, E. Morales, J. Root, I. Kumar, B. Garcia, C. Vellandi, D. Jenigian, T. Marsh, E. Henderson, and J. Vesenka, *J. Vac. Sci. Technol. A* 16, 1172 (1998).
143. A. J. Storm, J. van Noort, S. de Vries, and C. Dekker, *Appl. Phys. Lett.* 79, 3881 (2001).
144. K.-H. Yoo, D. H. Ha, J.-O Lee, J. W. Park, J. Kim, J. J. Kim, H.-Y. Lee, T. Kawai, and H. Y. Choi, *Phys. Rev. Lett.* 87, 198102 (2001).
145. H. Böttger and V. V. Bryksin, "Hopping Conduction in Solids." Akademie-Verlag, Berlin, 1985.
146. A. Yu. Kasumov, M. Kociak, S. Guéron, B. Reulet, V. T. Volkov, D. V. Klinov, and H. Bouchiat, *Science* 291, 280 (2001).
147. L. Cai, H. Tabata, and T. Kawai, *Appl. Phys. Lett.* 77, 3105 (2000).
148. T. Kanno, H. Tanaka, N. Miyoshi, and T. Kawai, *Jpn. J. Appl. Phys. 1* 39, 269 (2000).
149. T. Kanno, H. Tanaka, N. Miyoshi, and T. Kawai, *Appl. Phys. Lett.* 77, 3848 (2000).
150. T. Kanno, H. Tanaka, N. Miyoshi, M. Fukuda, and T. Kawai, *Jpn. J. Appl. Phys. 1* 39, 1892 (2000).
151. Y. Zhang, R. H. Austin, J. Kraeft, E. C. Cox, and N. P. Ong, *Phys. Rev. Lett.* 89, 198102 (2002).
152. K. W. Hipps, *Science* 294, 536 (2001).
153. X. D. Cui, A. Primak, X. Zarate, J. Tomfohr, O. F. Sankey, A. L. Moore, T. A. Moore, D. Gust, G. Harris, and S. M. Lindsay, *Science* 294, 571 (2001).
154. D. H. Ha, H. Nham, K.-H. Yoo, H. So, H.-Y. Lee, and T. Kawai, *Chem. Phys. Lett.* 355, 405 (2002).
155. H.-Y. Lee, H. Tanaka, Y. Otsuka, K.-H. Yoo, J.-O. Lee, and T. Kawai, *Appl. Phys. Lett.* 80, 1670 (2002).
156. D. N. Beratan, S. Priyadarshy, and S. M. Risser, *Chem. Biol.* 4, 3 (1997).
157. V. M. Orlov, A. M. Smirnov, and Y. M. Varshavsky, *Tetrahedron Lett.* 48, 4377 (1976).
158. C. A. M. Seidel, A. Schultz, and M. H. M. Sauer, *J. Phys. Chem.* 100, 5541 (1996).
159. S. Steenken and S. C. Jovanovic, *J. Am. Chem. Soc.* 119, 617 (1997).
160. N. S. Hush and A. S. Cheung, *Chem. Phys. Lett.* 34, 11 (1975).
161. H. Sugiyama and I. Saito, *J. Am. Chem. Soc.* 118, 7063 (1996).
162. I. Saito, T. Nakamura, K. Nakatani, Y. Yoshioka, K. Yamaguchi, and H. Sugiyama, *J. Am. Chem. Soc.* 120, 12686 (1998).
163. A.-O. Colson, B. Besler, M. D. Close, and M. D. Sevilla, *J. Phys. Chem.* 96, 661 (1992).
164. A.-O. Colson, B. Besler, and M. D. Sevilla, *J. Phys. Chem.* 96, 9787 (1992).
165. M. D. Sevilla, B. Besler, and A.-O. Colson, *J. Phys. Chem.* 99, 1060 (1995).

166. M. Hutter and T. Clark, *J. Am. Chem. Soc.* 118, 7574 (1996).
167. N. S. Kim and P. R. LeBreton, *J. Am. Chem. Soc.* 118, 3694 (1996).
168. H. Fernando, G. A. Papadantonakis, N. S. Kim, and P. R. LeBreton, *Proc. Natl. Acad. Sci. USA* 95, 5550 (1998).
169. F. Prat, K. N. Houk, and C. S. Foote, *J. Am. Chem. Soc.* 120, 845 (1998).
170. W. B. Davis, M. R. Wasielewski, M. A. Ratner, V. Mujica, and A. Nitzan, *J. Phys. Chem. A* 101, 6158 (1997).
171. Y. A. Berlin, A. L. Burin, and M. A. Ratner, *J. Phys. Chem. A* 104, 443 (2000).
172. Y. A. Berlin, A. L. Burin, and M. A. Ratner, *J. Am. Chem. Soc.* 123, 260 (2001).
173. Y. A. Berlin, A. L. Burin, L. D. A. Siebbeles, and M. A. Ratner, *J. Phys. Chem. A* 105, 5666 (2001).
174. Y. A. Berlin, A. L. Burin, and M. A. Ratner, *Chem. Phys.* 275, 61 (2002).
175. F. C. Grozema, L. D. A. Siebbeles, Y. A. Berlin, and M. A. Ratner, *Chem. Phys. Chem.* 3, 536 (2002).
176. Y. A. Berlin, A. L. Burin, and M. A. Ratner, *Superlattice Microstruct.* 28, 241 (2000).
177. X. Li and Y. Yan, *J. Chem Phys.* 115, 4169 (2001).
178. X. Li, H. Y. Zhang, and Y. Yan, *J. Phys. Chem. A* 105, 9563 (2001).
179. X. Li and Y. Yan, *Appl. Phys. Lett.* 79, 2190 (2001).
180. Y. Yan and H. Y. Zhang, *J. Theoretical Computational Chem.* 1, 225 (2002).
181. X. Y. Yu, H. Y. Zhang, P. Han, X. Li, and Y. Yan, *J. Chem. Phys.* 117, 2180 (2002).
182. J. Jortner, M. Bixon, T. Langenbacher, and M. E. Michel-Beyerle, *Proc. Natl. Acad. Sci. USA* 95, 12759 (1998).
183. M. Bixon, B. Giese, S. Wessely, T. Langenbacher, M. E. Michel-Beyerle, and J. Jortner, *Proc. Natl. Acad. Sci. USA* 96, 11713 (1999).
184. M. Bixon and J. Jortner, *J. Adv. Chem. Phys.* 106, 35 (1999).
185. M. Bixon and J. Jortner, *J. Phys. Chem. B* 104, 3906 (2000).
186. J. Jortner, M. Bixon, A. Voityuk, and N. Rösch, *J. Phys. Chem. A* 106, 7599 (2002).
187. A. A. Voityuk, N. Rösch, M. Bixon, and J. Jortner, *J. Phys. Chem. B* 104, 9740 (2000).
188. F. C. Grozema, Y. A. Berlin, and L. D. A. Siebbeles, *Int. J. Quantum Chem.* 75, 1009 (1999).
189. F. C. Grozema, Y. A. Berlin, and L. D. A. Siebbeles, *J. Am. Chem. Soc.* 122, 10903 (2000).
190. Y.-J. Ye, R. S. Chen, A. Martinez, P. Otto, and J. Ladik, *Solid State Commun.* 112, 139 (1999).
191. Y.-J. Ye, R. S. Chen, F. Chen, J. Sun, and J. Ladik, *Solid State Commun.* 119, 175 (2001).
192. L. Shen, Y.-J. Ye, and J. Ladik, *Solid State Commun.* 121, 35 (2002).
193. G. Brunaud, F. Castet, A. Fritsch, and L. Ducasse, *Phys. Chem. Chem. Phys.* 4, 6072 (2002).
194. D. Bicout and E. Kats, *Phys. Lett. A* 300, 479 (2002).
195. B. Giese, S. Wessely, M. Spormann, U. Lindemann, E. Meggers, and M. E. Michel-Beyerle, *Angew. Chem. Int. Ed.* 38, 996 (1999).
196. R. Bruinsma, G. Gruner, M. R. D. Orsogna, and J. Rudnick, *Phys. Rev. Lett.* 85, 4393 (2000).
197. E. W. Schlag, D.-Y. Yang, S.-Y. Sheu, H. L. Selzle, S. H. Lin, and P. M. Rentzepis, *Proc. Nat. Acad. Sci. USA* 97, 9849 (2000).
198. A. Voityuk, K. Siriwong, and N. Rösch, *Phys. Chem. Chem. Phys.* 3, 5421 (2001).
199. S. Komineas, G. Kalosakas, and A. R. Bishop, *Phys. Rev. E* 65, 061905-1 (2002).
200. W. Zhang, A. O. Govorov, and S. E. Ulloa, *Phys. Rev. B* 66, 060303(R) (2002).
201. Z. G. Yu and X. Song, *Phys. Rev. Lett.* 86, 6018 (2001).
202. R. G. Endres, D. L. Cox, R. R. P. Singh, and S. K. Pati, *Phys. Rev. Lett.* 88, 166601-1 (2002).
203. M. Zwolak and M. Di Ventra, *Appl. Phys. Lett.* 81, 925 (2002).
204. A. Yu. Kasumov, private communication.
205. G. Cuniberti, L. Craco, D. Porath, and C. Dekker, *Phys. Rev. B* 65, 241314(R) (2002).
206. D. Ly, Y. Kan, B. Armitage, and G. B. Schuster, *J. Am. Chem. Soc.* 118, 8747 (1996).
207. D. Ly, L. Sanii, and G. B. Schuster, *J. Am. Chem. Soc.* 121, 9400 (1999).
208. G. B. Schuster, *Acc. Chem. Res.* 33, 253 (2000).
209. B. Armitage, D. Ly, T. Koch, H. Frydenlund, H. Orum, H. G. Batz, and G. B. Schuster, *Proc. Natl. Acad. Sci. USA* 94, 12320 (1997).
210. E. M. Conwell and S. V. Rakhmanova, *Proc. Nat. Acad. Sci. USA* 97, 4556 (2000).
211. S. V. Rakhmanova and E. M. Conwell, *J. Phys. Chem. B* 105, 2056 (2001).
212. S. V. Rakhmanova and E. M. Conwell, *Appl. Phys. Lett.* 75, 1518 (1999).
213. V. D. Lakhno, *J. Biol. Phys.* 26, 133 (2000).
214. Z. Hermon, S. Caspi, and E. Ben-Jacob, *Europhys. Lett.* 43, 482 (1998).
215. E. B. Brauns, M. L. Madaras, R. S. Coleman, C. J. Murphy, and M. A. Berg, *J. Am. Chem. Soc.* 121, 11644 (1999).
216. Z. Liang, J. H. Freed, R. S. Keyes, and A. M. Bobst, *J. Phys. Chem. B* 104, 5372 (2000).
217. P. N. Borer, S. R. Pante, A. Kumar, N. Zanatta, A. Martin, A. Hakkinen, and G. C. Levy, *Biochemistry* 33, 2441 (1994).
218. R. N. Barnett, C. L. Cleveland, A. Joy, U. Landman, and G. B. Schuster, *Science* 294, 567 (2001).
219. M. Hjort and S. Stafstrom, *Phys. Rev. Lett.* 87, 228101 (2001).
220. Y. Eichen, E. Braun, U. Sivan, and G. Ben-Yoseph, *Acta Polym.* 49, 663 (1998).
221. W. Pompe, M. Mertig, R. Kirsch, R. Wahl, L. C. Ciacchi, J. Richter, R. Seidel, and H. Vinzelberg, *Z. Metallkd.* 90, 1085 (1999).
222. J. Richter, R. Seidel, R. Kirsch, M. Mertig, W. Pompe, J. Plaschke, and H. K. Schackert, *Adv. Mater.* 12, 507 (2000).
223. J. Richter, *Physica E*, in press
224. J. Richter, M. Mertig, W. Pompe, and H. Vinzelberg, *Appl. Phys. A* 74, 725 (2002).
225. O. Harnack, W. E. Ford, A. Yasuda, and J. M. Wessels, *Nano Lett.* 2, 919 (2002).
226. W. E. Ford, O. Harnack, A. Yasuda, and J. M. Wessels, *Adv. Mater.* 13, 1793 (2001).
227. F. Patolsky, Y. Weizmann, O. Lioubashevski, and I. Willner, *Angew. Chem. Int. Ed.* 41, 2323 (2002).
228. M. Mertig, L. C. Ciacchi, R. Seidel, W. Pompe, and A. De Vita, *Nano Lett.* 2, 841 (2002).
229. A. Kumar, M. Pattarkine, M. Bhadbhade, A. B. Mandale, K. N. Ganesh, S. S. Datar, C. V. Dharmadhikari, and M. Sastry, *Adv. Mater.* 13, 341 (2001).
230. M. Sastry, A. Kumar, S. Datar, C. V. Dharmadhikari, and K. N. Ganesh, *Appl. Phys. Lett.* 78, 2943 (2001).
231. A. Rakitin, P. Aich, C. Papadopoulos, Yu. Kobzar, A. S. Vedeneev, J. S. Lee, and J. M. Xu, *Phys. Rev. Lett.* 86, 3670 (2001).
232. P. Aich, S. L. Labiuk, L. W. Tari, L. J. T. Delbaere, W. J. Roesler, K. J. Falk, R. P. Steer, and J. S. Lee, *J. Mol. Biol.* 294, 477 (1999).
233. J. S. Lee, L. J. P. Latimer, and R. S. Reid, *Biochem. Cell Biol.* 71, 162 (1993).
234. P. Aich, H. B. Kraatz, and J. S. Lee, *J. Biomol. Struct. Dyn., Sp. Iss.* S2, 297 (2000).
235. P. Aich, R. J. S. Skinner, S. D. Wettig, R. P. Steer, and J. S. Lee, *J. Biomol. Struct. Dyn.* 20, 93 (2002).
236. E. Ben-Jacob, Z. Hermon, and S. Caspi, *Phys. Lett. A* 263, 199 (1999).
237. E. Winfree, F. Liu, L. A. Wenzler, and N. C. Seeman, *Nature* (*London*) 394, 539 (1998).
238. C. Mao, W. Sun, and N. C. Seeman, *J. Am. Chem. Soc.* 121, 5437 (1999).

239. F. Liu, R. Sha, and N. C. Seeman, *J. Am. Chem. Soc.* 121, 917 (1999).
240. C. Mao, W. Sun, and N. C. Seeman, *Nature* (*London*) 386, 137 (1997).
241. J. Chen and N. C. Seeman, *Nature* (*London*) 350, 631 (1991).
242. C. Mao, T. H. LaBean, J. H. Reif, and N. C. Seeman, *Nature* (*London*) 407, 493 (2000).
243. C. Mao, W. Sun, Z. Shen, and N. C. Seeman, *Nature* (*London*) 397, 144 (1999).
244. B. Yurke, A. J. Turberfield, A. P. Mills, Jr., F. C. Simmel, and J. L. Neumann, *Nature* (*London*) 406, 605 (2000).
245. I. Willner and B. Willner, *Pure Appl. Chem.* 74, 1753 (2002).
246. M. Sastry, *Pure Appl. Chem.* 74, 1609 (2002).
247. C. J. Nulf and D. R. Corey, *Nucleic Acids Res.* 30, 2782 (2002).
248. D. L. Feldheim and C. D. Keating, *Chem. Soc. Rev.* 27, 1 (1998).
249. C. M. Niemeyer and M. Alder, *Angew. Chem. Int. Ed.* 41, 3779 (2002).
250. R. Bashir, *Superlattices Microstruct.* 29, 1 (2001).
251. C. A. Mirkin, R. L. Letsinger, R. C. Mucic, and J. J. Stofhoff, *Nature* (*London*) 382, 607 (1996).
252. A. P. Alivisatos, K. P. Johnson, T. E. Wilson, C. J. Loveth, M. P. Bruchez, and P. G. Schultz, *Nature* (*London*) 382, 609 (1996).
253. D. Bethell and D. J. Schiffrin, *Nature* (*London*) 382, 581 (1996).
254. Y. Shao, Y. Jin, and S. Dong, *Electrochem. Commun.* 4, 773 (2002).
255. C. M. Niemeyer, *Science* 297, 62 (2002).
256. M. Sastry, *Curr. Sci.* 79, 1089 (2000).
257. J. H. Fendler, *Chem. Mater.* 8, 1616 (1996).
258. S. Henrichs, C. P. Collier, R. J. Saykally, and J. R. Heath, *J. Am. Chem. Soc.* 122, 4077 (2000).
259. R. L. Whetten, J. T. Khoury, M. M. Alvarez, S. Murthy, I. Vezmar, Z. L. Wang, P. W. Stephens, C. L. Cleveland, W. D. Luedtke, and U. Landman, *Adv. Mater.* 8, 428 (1996).
260. J. Fink, C. S. Kiely, D. Bethell, and D. J. Schiffrin, *Chem. Mater.* 10, 922 (1998).
261. N. C. Seeman, *Annu. Rev. Biophys. Biomol. Struct.* 27, 225 (1998).
262. G. P. Lopinski, D. D. M. Wayner, and R. A. Wolkow, *Nature* (*London*) 406, 48 (2000).
263. R. H. Austin, J. P. Brody, E. C. Cox, K. Duke, and W. Volkmuth, *Phys. Today* 50, 32 (1997).
264. C. A. Mirkin and T. A. Taton, *Nature* (*London*) 405, 626 (2000).
265. J. L. Coffer, S. R. Bigham, X. Li, R. F. Pinizzotto, Y. G. Rho, R. M. Pirtle, and I. L. Pirtle, *Appl. Phys. Lett.* 69, 3851 (1996).
266. K. Keren, M. Krueger, R. Gilad, G. Ben-Yoseph, U. Sivan, and E. Braun, *Science* 297, 72 (2002).
267. J. K. N. Mbindyo, B. D. Reiss, B. R. Martin, C. D. Keating, M. J. Natan, and T. E. Mallouk, *Adv. Mater.* 13, 249 (2001).
268. S. J. Xiao, F. R. Liu, A. E. Rosen, J. F. Hainfeld, N. C. Seeman, K. Musier-Forsyth, and R. A. Kiehl, *J. Nanopart. Res.* 4, 313 (2002).
269. D. M. Hartmann, M. Heller, S. C. Esener, D. Schwartz, and G. Tu, *J. Mater. Res.* 17, 473 (2002).
270. J. L. Coffer, S. R. Bigham, R. F. Pinizzotto, and H. Yang, *Nanotechnology* 3, 69 (1992).
271. S. R. Bigham and J. L. Coffer, *Colloids Surf. A* 95, 211 (1995).
272. J. L. Coffer, *J. Cluster Sci.* 8, 159 (1997).
273. C. M. Niemeyer, W. Burger, and J. Peplies, *Angew. Chem. Int. Ed.* 37, 2265 (1998).
274. S.-J. Park, A. A. Lazarides, C. A. Mirkin, and R. L. Letsinger, *Angew. Chem. Int. Ed.* 40, 2909 (2001).
275. M. A. Batalia, E. Protozanova, R. B. Macgregor, and D. A. Erie, *Nano Lett.* 2, 269 (2002).
276. R. C. Mucic, J. J. Storhoff, C. A. Mirking, and R. L. Letsinger, *J. Am. Chem. Soc.* 120, 12674 (1998).
277. G. P. Mitchell, C. A. Mirkin, and R. L. Letsinger, *J. Am. Chem. Soc.* 121, 8122 (1999).
278. J. J. Storhoff, A. A. Lazarides, C. A. Mirkin, R. L. Letsinger, R. C. Mucic, and G. C. Schatz, *J. Am. Chem. Soc.* 122, 4640 (2000).
279. S.-J. Park, A. A. Lazarides, C. A. Mirkin, P. W. Brazis, C. R. Kannewurf, and R. L. Letsinger, *Angew. Chem. Int. Ed.* 39, 3845 (2000).
280. C. M. Niemeyer, M. Alder, S. Lenhert, S. Gao, H. Fuchs, and L. Chi, *Chem. Bio. Chem.* 2, 260 (2001).
281. C. Dwyer, M. Guthold, M. Falvo, S. Washburn, R. Superfine, and D. Erie, *Nanotechnology* 13, 601 (2002).
282. A. R. Pike, L. H. Lie, R. A. Eagling, L. C. Ryder, S. N. Patole, B. A. Connolly, B. R. Horrocks, and A. Houlton, *Angew. Chem. Int. Ed.* 41, 615 (2002).
283. A. Pike, B. Horrocks, B. Connolly, and A. Houlton, *Aust. J. Chem.* 55, 191 (2002).
284. L. M. Demers, D. S. Ginger, S.-J. Park, Z. Li, S.-W. Chung, and C. A. Mirkin, *Science* 296, 1836 (2002).